Lawrence Berkeley National Laboratory
Joint Genome Institute

Title
Genetic mapping and prediction of flowering time and plant height in a maize Stiff Stalk MAGIC population

Permalink
https://escholarship.org/uc/item/9068q5kw

Journal
Genetics, 221(2)

ISSN
0016-6731

Authors
Michel, Kathryn J
Lima, Dayane C
Hundley, Hope
et al.

Publication Date
2022-05-31

DOI
10.1093/genetics/iyac063

Peer reviewed

OXFORD GENETICS

Genetic mapping and prediction of flowering time and plant height in a maize Stiff Stalk MAGIC population

Kathryn J. Michel [ID],[1] Dayane C. Lima [ID],[1] Hope Hundley [ID],[2] Vasanth Singan [ID],[2,†] Yuko Yoshinaga [ID],[2] Chris Daum [ID],[2] Kerrie Barry [ID],[2] Karl W. Broman [ID],[3] C. Robin Buell [ID],[4,5,‡] Natalia de Leon [ID],[1,6] Shawn M. Kaeppler [ID] [1,6,7,*]

[1]Department of Agronomy, University of Wisconsin—Madison, Madison, WI 53706, USA,
[2]U.S. Department of Energy Joint Genome Institute, Berkeley, CA 94720, USA,
[3]Departments of Biostatistics and Medical Informatics, University of Wisconsin–Madison, WI 53706, USA,
[4]Department of Plant Biology, Michigan State University, East Lansing, MI 48824, USA,
[5]Department of Energy, Great Lakes Bioenergy Research Center, Michigan State University, East Lansing, MI 48824, USA,
[6]Department of Energy, Great Lakes Bioenergy Research Center, University of Wisconsin—Madison, Madison, WI 53706, USA,
[7]Wisconsin Crop Innovation Center, University of Wisconsin—Madison, Middleton, WI 53562, USA

*Corresponding author: Department of Agronomy, University of Wisconsin—Madison, 1575 Linden Dr., Madison, WI 53706, USA. Email: smkaeppl@wisc.edu
†Present address: Ambry Genetics, 1 Enterprise, Aliso Viejo, CA 92656, USA.
‡Present address: Department of Crop and Soil Sciences, Center for Applied Genetic Technologies, University of Georgia, Athens, GA 30602, USA.

Abstract

The Stiff Stalk heterotic pool is a foundation of US maize seed parent germplasm and has been heavily utilized by both public and private maize breeders since its inception in the 1930s. Flowering time and plant height are critical characteristics for both inbred parents and their test crossed hybrid progeny. To study these traits, a 6-parent multiparent advanced generation intercross population was developed including maize inbred lines B73, B84, PHB47 (B37 type), LH145 (B14 type), PHJ40 (novel early Stiff Stalk), and NKH8431 (B73/B14 type). A set of 779 doubled haploid lines were evaluated for flowering time and plant height in 2 field replicates in 2016 and 2017, and a subset of 689 and 561 doubled haploid lines were crossed to 2 testers, respectively, and evaluated as hybrids in 2 locations in 2018 and 2019 using an incomplete block design. Markers were derived from a practical haplotype graph built from the founder whole genome assemblies and genotype-by-sequencing and exome capture-based sequencing of the population. Genetic mapping utilizing an update to R/qtl2 revealed differing profiles of significant loci for both traits between 635 of the DH lines and 2 sets of 570 and 471 derived hybrids. Genomic prediction was used to test the feasibility of predicting hybrid phenotypes based on the per se data. Predictive abilities were highest on direct models trained using the data they would predict (0.55–0.63), and indirect models trained using per se data to predict hybrid traits had slightly lower predictive abilities (0.49–0.55). Overall, this finding is consistent with the overlapping and nonoverlapping significant quantitative trait loci found within the per se and hybrid populations and suggests that selections for phenology traits can be made effectively on doubled haploid lines before hybrid data is available.

Keywords: maize; quantitative trait loci; genomic prediction; multiparent population; MPP; Multiparental Populations; Multiparent Advanced Generation Inter-Cross (MAGIC)

Introduction

Multiparent mapping populations are an effective tool for discovering quantitative trait loci (QTL) in plant and animal species. Multiparent advanced generation intercross (MAGIC) populations offer a powerful QTL mapping structure because intercrossing more than 2 parents increases genetic diversity while managing minor allele frequency and reducing haplotype length through recombination (reviewed in Scott *et al.* 2020). MAGIC populations have been used to successfully dissect the genetic control of complex traits in various plant species, including *Arabidopsis* (Kover *et al.* 2009), maize (Dell'Acqua *et al.* 2015), rice (Ogawa *et al.* 2018), barley (Sannemann *et al.* 2015), wheat (Gardner *et al.* 2016), sorghum (Ongom and Ejeta 2018), tomato (Pascual *et al.* 2015), and cowpea (Huynh *et al.* 2018). Multiparent populations balance the advantages and disadvantages of biparental mapping

populations and association panels. Geneticists often rely on the cross of 2 individuals with contrasting phenotypes to generate a population of segregating individuals and then perform linkage analysis to associate genetic loci with the trait of interest. Recently, increased marker density due to technological advancements and rapidly declining genotyping costs allowed researchers to evaluate diverse association panels to assay historical recombination to find associations between markers and phenotypes (reviewed in Tibbs Cortes *et al.* 2021). Despite the success of these methods, both techniques face intrinsic challenges. Biparental populations rely on the genetic diversity found in just 2 parents, which can limit the scope of discovered QTLs to the backgrounds studied. Association panels often contain rare alleles that do not meet the minor allele frequency threshold and are discarded due to low statistical power associated with such

rarity. Thus, MAGIC populations seek to balance these characteristics by incorporating more than 2 genetic backgrounds while balancing minor allele frequency and increasing mapping resolution (Kover et al. 2009; Romay et al. 2013; Dell'Acqua et al. 2015).

To study the genetic architecture of traits relevant to maize hybrid performance and adaptation, we developed a MAGIC population from 6 inbred lines spanning the diversity of the Stiff Stalk heterotic pool. The Stiff Stalk heterotic group was founded in the Iowa Stiff Stalk Synthetic (BSSS) breeding population, which was initiated during the 1930s by Dr George Sprague to improve stalk quality, yield, and agronomic quality of maize inbreds (Troyer 2004). Several key inbreds were released out of BSSS, including B14 in 1953, B37 in 1958, B73 in 1972, and B84 in 1979 (Russell 1972, 1979; Troyer 1999). Since their release, these founder BSSS inbreds have been used extensively by breeders in the public and private sectors in the USA, and the Stiff Stalk group has become the de facto source of seed parent germplasm for many hybrid breeding programs. It is estimated that B73, B14, and B37 contributed conservatively 16.4% to germplasm released by Monsanto Company, Pioneer Hi-Bred, International (PHI), and Syngenta between 2004 and 2008 (Mikel 2011). In a group of 1,506 lines released under plant variety protection (PVP) certificates between the year 2000 and 2019, researchers found that one-third of the lines had kinship estimated Stiff Stalk admixture >30%, and 15% of lines had Stiff Stalk admixture >50% (White et al. 2020). Thus, the Stiff Stalk heterotic group remains a vital source of commercial maize germplasm in North America. This research utilized 6 Stiff Stalk inbreds—B73, B84, NKH8431, LH145, PHB47, and PHJ40—that represent key founders in commercial breeding programs. Recent work reported the genome sequences of these inbreds (excluding B73) and found extensive genomic variation between B73 and the other 5 parents along with conservation of base BSSS haplotypes within each inbred (Bornowski et al. 2021).

Throughout the process of developing new inbred lines and hybrid varieties, maize breeders balance selecting for hybrid yield with other traits needed for successful inbred and hybrid seed production. Traits such as flowering time and plant height are vital to the success of an inbred within the breeding program and as a parent to a successful hybrid variety. Extensive research has been conducted on maize flowering time, including the discovery of a multitude of small to large effect QTL contributing to flowering time and photoperiod sensitivity variation in maize (Buckler et al. 2009; Xu et al. 2012; Wang et al. 2021) and the identification of several genes and regulatory elements involved in the pathway, including ID1, DLF1, ZmCCA1, ZmMADS1, ZmCOL3, Vgt1, ZCN8, ZmCCT, ZmCCT9, ZmCCT10, and ZmMADS69 (Colasanti et al. 1998; Muszynski et al. 2006; Salvi et al. 2007; Wang et al. 2011; Hung et al. 2012; Alter et al. 2016; Guo et al. 2018; Huang et al. 2018; Jin et al. 2018; Liang et al. 2019; Stephenson et al. 2019). Flowering time and photoperiod sensitivity are determinants of maize yield because the combination leads to adaptation of maize lines to their intended environments, such that tropical lines with daylight sensitivity must undergo extensive selection for adaptation to succeed in northern regions that do not meet daylight needs of tropical plants (Xu et al. 2012). In addition, timing of flowering can influence the total length of time available for grain filling post flowering and the ability of a hybrid to mature within a frost-free seasonal interval. Within an environment, maize hybrids with full-season relative maturities often yield more than their shorter-season counterparts, and timing of planting date to achieve flowering time before environment specific cutoffs is vital for maximizing yield potential (Baum et al. 2019). However, later-maturing varieties can face risk due to early frosts and susceptibility to seasonal drought effects (Duvick and Cassman 1999), therefore plant breeders need to carefully balance flowering time and total maturity to suit their target population of environments to maximize maize grain yield. In maize hybrid varieties, flowering time typically exhibits heterosis where the hybrid flowers sooner than the earlier of the 2 inbred parents, as demonstrated by a partial diallel of ex-PVP inbreds (Li et al. 2018) and an association panel of 302 diverse inbreds crossed to B73 (Flint-Garcia et al. 2009).

Like flowering time, substantial efforts have been devoted to understand the genetic underpinnings of maize plant and ear height. Major mutations in the gibberellin and brassinosteroid pathways affecting height have been identified in addition to numerous QTL (reviewed by Salas Fernandez et al. 2009). Despite its high heritability, QTL affecting height tend to have very small effects, with the largest effect in the maize United States-Nested Association Mapping (US-NAM) population explaining $2.1 \pm 0.9\%$ of the variation, which suggests that maize height follows an infinitesimal model of inheritance (Peiffer et al. 2014). In addition, identification of QTL can depend on environmental conditions such as drought and nutrient stress, which may reduce the relative proportion of additive genetic variance compared with genotype by environment and error variance (Cai et al. 2012; Wallace et al. 2016). In general, taller plants can face increased root and stalk lodging pressure due to the proportionally higher placement of the ear on the stalk, which increases the ear's leverage during wind events or disease pressure. During the Green Revolution, major yield gains were made in rice and wheat by decreasing overall plant height, which reduced the risk of lodging under more intensive agricultural management (reviewed by Khush 2001). Maize breeders consider height selection in both inbreds and hybrids, as lodging can make harvest difficult and inefficient for both seed parents and commercial varieties. Due to heterosis, the hybrid is usually taller than the taller of the 2 inbred parents, as shown in a partial diallel of ex-PVP inbreds (Li et al. 2018) and in an association panel of 302 diverse lines crossed to B73 (Flint-Garcia et al. 2009).

The main objectives of this work are to: (i) report a MAGIC population based on the Stiff Stalk heterotic group and its associated genetic and phenotypic resources; (ii) dissect the genetic architecture of flowering time and plant height within the per se population of DH lines and 2 test cross populations; and (iii) perform genomic prediction to investigate the relationship between per se and hybrid phenotypes.

Materials and methods
Population development
Inbreds B73, B84, NKH8431, LH145, PHB47, and PHJ40 were chosen to represent the primary Stiff Stalk subheterotic groups (Table 1; White et al. 2020). Biographical information for each line was obtained from the Germplasm Resource Information Network (GRIN) database (npgsweb.ars-grin.gov). The inbreds B73 and B84 were released from the BSSS in cycles 5 and 7, respectively, and B84 contains resistance to Helminthosporium turcicum ("Ht" currently known as Setosphaeria turcica, common name Northern Corn Leaf Blight). Inbred LH145 was developed by Holden's Foundation Seed, Inc. (acquired by Monsanto Company in 1997) from the cross of A632Ht and CM105, both of which have B14 as a parent. Inbred NKH8431 was developed from 1 B73 derived line and 2 B14 derived lines by Northrup, King & Company. Inbreds PHB47 and PHJ40 were both released by PHI. Inbred PHB47 was made from a cross between B37 and SD105, with 2

Table 1. Origins of Stiff Stalk inbred lines.

Line	Originator	Subheterotic group	PI number
B73	Iowa State University	B73	PI 550473
B84	Iowa State University	B73	PI 608767
LH145	Holden's Foundation Seed, Inc.	B14	PI 600959
NKH8431 (alias H8431, NPH8431)	Northrup, King & Company	B14	PI 601610
PHB47 (alias B47)	Pioneer Hi-Bred International, Inc.	B37	PI 601009
PHJ40	Pioneer Hi-Bred International, Inc.	Flint	PI 601321

Subheterotic groupings from White *et al.* (2020).

backcrosses to B37 before inbred development. Inbred PHJ40 is an early flowering flint and Stiff Stalk line developed in Ontario, Canada, with previously demonstrated admixture with B37 (White *et al.* 2020). All inbred lines except B73 previously underwent whole genome, reference guided assembly, which revealed extensive genetic and genomic diversity between the 5 lines and B73 (Bornowski *et al.* 2021).

The population, named WI-SS-MAGIC, was initiated at a winter nursery during winter 2007. A detailed timeline of the population development is presented in Supplementary File 1. Briefly, the 6 parents were crossed in a half diallel and then every possible F_1 hybrid combination cross (without reciprocals) was attempted. In the infrequent event that a cross of 2 F_1 plants failed, additional seeds from other crosses were included in the balanced bulk to maintain equal representation of all parents. Random intermating was performed between rows by designating plants as either a pollen parent or seed parent and using the individual only once for crossing. The intermating process utilized a minimum of 200 plants producing a minimum of 100 harvested ears per generation. Balanced bulks were made after harvesting the intermated plants. After 2 generations of intermating, a subset of the population (hereafter "Subset A") was sent for doubled haploid (DH) induction, provided as in-kind support by AgReliant Genetics. The remaining balanced bulk was randomly intermated for 2 additional generations and then sent for DH induction (hereafter "Subset B"). Individuals in Subset A were given coded names beginning with W10004 and numbered from 1 to N, where N is the number of individuals (i.e. W10004_0001 through W10004_04xx), and individuals in Subset B were named using W10004 and a number from 500 to 500 + N, where N is the number of individuals returned (i.e. W10004_0500 through W10004_xxxx) (Supplementary Table 1).

Collection of per se DH line phenotypic data

A set of 779 DH lines was planted during summers 2016 and 2017 at the West Madison Agricultural Research Station in Verona, WI (Supplementary Table 1). Subset A and B groups were organized as subblocks within a randomized complete block design with 2 replications. Parents were included as checks in both subblocks. Both trials were planted in fields that followed soybeans in the previous year and were managed with standard agronomic practices. Detailed information about planting dates and densities, soil types, and nutrient and pesticide management is presented in Supplementary Table 2. Three representative plants per plot were measured for plant and ear height. Plant height was measured as the height from the ground, in centimeters, to the collar of the flag leaf, while ear height was the height, in centimeters, from the ground to the base of the node subtending the uppermost ear. Growing degree units to anthesis and silking were measured on a whole plot basis (AnthGDU and SilkGDU, respectively). Anthesis and silking were measured as the number

of days from planting it took to observe approximately 50% of the plants in the plot to reach pollen shed and silk extrusion, respectively. Dates were converted to growing degree units using a base temperature of 50F and maximum temperature of 86F (Pope 2008) using temperature data obtained from the weather station located at the University of Wisconsin (UW) West Madison Agricultural Research Station to standardize for differential daily heat unit accumulation across years. Since lines developed through doubled haploidy are expected to be genetically uniform, lines with observable phenotypic segregation were discarded. Severely lodged plants were not evaluated for height characteristics. To remove outlier data points, individual plant measurements were discarded if the ear height to plant height measurement ratio was <0.25 or >0.75, and whole plot ear or plant height measurements were discarded if the within plot variance was >500 cm^2.

Generation of hybrids and collection of phenotypic data

Hybrid seed was produced by crossing the WI-SS-MAGIC population to PHJ89 and DKH3IIH6 (hereafter 3IIH6). The hybrid populations were named SS-PHJ89 and SS-3IIH6. PHJ89 is an Oh43-type inbred line developed by Pioneer Hi-Bred (White *et al.* 2020). The inbred 3IIH6 is an Iodent-type inbred line developed by DeKalb Genetics Corporation (acquired by Monsanto in 1998, now owned by Bayer AG) through selfing the F_1 Hybrid PHI3737 (Dekalb Plant Genetics 1994). PHJ89 and 3IIH6 are related by pedigree through their founder PHG47, which is one of the 2 parents of PHJ89 and one of the parents of hybrid variety PH3737 from which 3IIH6 was generated through selfing, so they are expected to contain regions of identity by descent (Pioneer Hi-Bred International Inc. 1992; Mikel 2011). Hybrids were grown during summers 2018 and 2019 at the UW West Madison Agricultural Research Station in Verona, Wisconsin and at the UW Arlington Research Station in Arlington, WI. Hybrids were blocked by tester, and each block included at least 5 replicates each of 2 commercial hybrids (DKC50-08RIB and DKC54-38RIB) and 2 replicates of each respective population parent–tester combination, when seed was available. All trials were incompletely replicated, where each hybrid genotype was grown at least once in each experiment with a consistent random subset replicated a second time. A total of 689 SS-3IIH6 hybrids were grown, of which 316 were replicated, while a total of 561 SS-PHJ89 hybrids were grown, of which 377 were replicated (Supplementary Table 1). The same set of replicated and unreplicated lines were grown across years and locations, with unique plot randomizations for each year–location combination. Replicated hybrids were randomized among the unreplicated hybrids within their respective tester blocks. All trials were planted in fields that followed soybeans in the previous year and were managed with standard agronomic practices. Detailed information about planting dates and densities, soil types, and

nutrient and pesticide management is presented in Supplementary Table 2. Flowering time growing degree units were recorded in the same manner as previously described for the per se population using weather data obtained from each research station. Flowering time was recorded for all hybrid plots in West Madison and for ~36% and 33% of hybrid plots in Arlington in 2018 and 2019, respectively. Plant height and ear height were measured on 3 competitive plants per plot for all plots. Stand counts were recorded manually, and plots were discarded if they contained fewer than 20 plants. The 2019 West Madison trial experienced extremely wet and cold germination conditions, which led to low stand counts for the SS-3IIH6 block. Only 19% and 38% of the plots had stands greater than 50 and 40 plants, respectively, which prompted us to discard the height data due to inconsistent interplant competition but keep flowering time data due to good correlations with flowering time from the previous year. To remove outlier data points, individual plant measurements were discarded if the ear height to plant height measurement ratio was <0.25 or >0.75, and whole plot height measurements were discarded if the within plot variance was >500 cm². Plot average height measurements and flowering GDU measurements that were more than 3 SDs away from the experiment wide mean were discarded.

Analysis of phenotypic data

A 2-stage approach was taken to analyze plot mean phenotypic data (Supplementary Table 3). In stage 1, following the procedures of Rogers et al. (2021), linear mixed models were fit using R/ASReml version 4 (Butler et al. 2017; R Core Team 2018) for each population within each environment using genotype as a fixed effect and replicate as a random effect. Next, models were fit with all combinations of autoregressive first order (AR1) and IID residual covariance structures of the x and y grid coordinates of the plot locations to account for spatial variation. The model with the lowest Schwarz's Bayesian Information Criterion (Schwarz 1978) was chosen to represent the environment, and the best linear unbiased estimators (BLUEs) and SEs were extracted from the model (Supplementary Table 4). Due to our incomplete block structure, the residual spatial correlations were restricted to $-0.6 < r < 0.6$. Any models with correlation outside this range were reset to using no residual covariance structure. In stage 2, genotypes were fit as fixed effects and environment and genotype by environment interaction terms were set as random effects. To weight the second stage analysis, the reciprocals of the first stage BLUE SEs were carried forward, which represent the genotype by replication interactions, and the unit's variance was constrained to 1. Within each experiment, any phenotypic BLUE that fell outside 2.5 times the interquartile range (IQR) was discarded as an outlier. Following the data cleaning described in the previous sections and the post hoc cleaning based on IQR, BLUEs were calculated for 730 DH lines, 658 SS-3IIH6 hybrids, and 535 SS-PHJ89 hybrids. Parental check lines were included in the analysis because they constitute the same population as the experimental lines, while commercial check hybrids were not included in the analysis. To estimate variance components and calculate heritability, the same model was used except genotype was set as a random effect. Heritability was calculated as follows (Cullis et al. 2006):

$$h^2_{\text{Cullis}} = 1 - \text{PEV}/2\sigma^2_g \qquad (1)$$

using the prediction error variance (PEV) and genetic variance (σ^2_g) obtained from the stage 2 analysis. To compare phenotypic variances across populations, the squared coefficient of variation was calculated to correct for the differences in scale between per se and hybrid phenotypes (Falconer and Mackay 1989). Pearson's correlations within and between phenotypes were calculated on trait BLUE values within and between the DH and 2 hybrid populations.

Genetic data
Sequencing using exome capture
Exome capture sequencing was performed on 701 DH lines from the WI-SS-MAGIC (Supplementary Table 1) using a custom capture design acquired from Roche Diagnostics Corporation (Indianapolis, IN). Probes were designed to target the 5' and 3' ends of the untranslated regions (UTRs) of the maize B73_RefGen_v2 genic regions and presence absence variation (PAV) regions derived from alignment of whole-genome sequencing reads of a core set of 32 inbreds to B73 reference version 2 (Brohammer et al. 2018; Mazaheri et al. 2019). In total, 82,351 genic regions (~26.5 Mb) and 492 PAV regions (~2.8 Mb) of the maize genome were targeted using tiled, variable length probes, with an average probe size of 75 nt (Supplementary File 2). Any overlapping regions were collapsed into a single target. The target regions ranged in size from 50 to 49,777 nucleotides (nt), with a mean size of 353.6 nt (Supplementary File 3). Briefly, DNA was extracted using seedling tissue using a modified CTAB method (Saghai-Maroof et al. 1984), sheared, and hybridized with adapters prior to SeqCap EZ solution capture, as previously described (Mascher et al. 2013) (Supplementary File 1). DNA was then amplified, enrichment quality control performed, and libraries sequenced by the US Department of Energy Joint Genome Institute (JGI) in paired end mode on the Illumina HiSeq 2500. Raw sequence quality was evaluated using FastQC v0.11.5 (https://www.bioinformatics.babraham.ac.uk/projects/fastqc) and MultiQC v1.0 (Ewels et al. 2016). Reads were then trimmed, low quality bases removed, and adapters removed using Cutadapt v1.14 (Martin 2011) with the following parameters: –length 150, -m 20, -q 20, 20, –times 2, and -g/-a/-G/-A along with their respective adapter sequences. After cleaning, read quality and adapter content were evaluated again using FastQC v.0.11.5 and MultiQC v1.0.

Genotyping by sequencing
Additional genotyping was performed on 144 DH lines using Genotyping-by-Sequencing (GBS) at the University of Wisconsin Biotechnology Center (Supplementary Table 1). Briefly, dual digest GBS was performed with restriction enzymes PstI and MspI on DNA extracted from frozen seedling leaf tissue (Elshire et al. 2011; Poland et al. 2012). DNA was sequenced using an Illumina NovaSeq6000 in paired end mode 150 nt and analyzed using bcl2fastq v2.20.0.422 (San Diego, CA, USA). Read 1 was demultiplexed and barcodes were removed using Tassel-5-Standalone plugin "ConvertOldFastqToModernFormatPlugin" with parameters "-e PstI-MspI" and "-p R1" (Bradbury et al. 2007). Read 2 was not included in future analysis.

Practical haplotype graph
A practical haplotype graph (PHG) (version 0.0.30) was built using B73 v5 as the reference (Bradbury et al. 2021, maizegdb.org). The B73 RefGen_v5 annotation of genes (Zm-B73-REFERENCE-NAM-5.0_Zm00001eb.1.gff3, available at maizegdb.org) was used to make the initial reference ranges, which were supplied to the "CreateValidIntervalsFilePlugin" to collapse any overlapping ranges and format for input into PHG. B73 RefGen_v5 was loaded as the

reference assembly using the "MakeInitialPHGDBPipelinePlugin," followed by the other 5 parental de novo genome assemblies using the "AssemblyHaplotypesMultiThreadPlugin" (Bornowski et al. 2021). The "AssemblyHaplotypesMultiThreadPlugin" uses mummer4 to align each assembly to the reference by chromosome in parallel (Marçais et al. 2018). Next, B73 was added to the graph using the "AddRefRangeAsAssemblyPlugin" which allows B73 haplotypes to be included as potential parental sequences.

A ranking file was generated by counting the number of haplotypes found within each assembly. The ranking file is necessary when 2 or more haplotypes are collapsed into a consensus haplotype, where the sequence of the highest-ranking line will represent the group. Consensus haplotypes were made using the PHG shell script "CreateConsensi.sh" with parameters "mxDiv = 0.0001" and "minTaxa = 1". All other parameters were left as default. The value of "mxDiv = 0.0001" was chosen such that genic regions would only be collapsed if they were truly identical, since over 90% of maize gene models are shorter than 10,000 bp. After consensus haplotypes were generated, the "ImputePipelinePlugin" with parameter "-imputeTarget pathToVCF" was used to index the pangenome, map exome capture and GBS reads to the graph, use a Hidden Markov Model (HMM) to find paths through the graph for each taxon, and call SNPs in the genic reference regions for the progeny population. The "minReads" parameter was set to zero to allow imputation of the paths using the aligned exome capture and GBS reads. Exome capture reads were aligned as paired end sequences, while the GBS reads were aligned as single end sequences. Parental assembly genic SNPs were extracted from the graph using the "FilterGraphPlugin" and "PathsToVCFPlugin." Due to the expected homozygosity of the DH lines and parental assemblies, only homozygous SNPs were generated from the PHG.

Markers were filtered and selected for mapping using Tassel-5-Standalone (Bradbury et al. 2007). The combined file of parental and population individuals (Supplementary File 4) was filtered to remove any non-Stiff Stalk individuals that were included as checks, SNPs with any missing parental data were removed, minor SNP states were set to missing to remove third, fourth, and other alleles, and the SNP was removed if the minor allele frequency was <0.05. To reduce correlation between SNPs and decrease QTL mapping computational time, 100,000 evenly spaced SNPs were selected across the 10 chromosomes and converted to numerical major or minor alleles. The SNP markers generated for the DH lines were also used for the derived hybrids, as we did not have genetic information on the testers.

Population genetic characteristics

Multidimensional scaling (MDS) was performed using 1.8 million unfiltered genic SNPs to confirm lack of population structure. A distance matrix was calculated using the "DistanceMatrixPlugin" from Tassel-5-Standalone with default parameters (Bradbury et al. 2007). In R, cmdscale() was used to calculate classical MDS on the distance matrix for the first 2 dimensions (R Core Team 2018). Allele frequencies were calculated on the set of 100,000 SNPs used for QTL mapping.

QTL mapping

Quality control analyses, single-marker QTL mapping, and SNP associations were performed using R/qtl2 with the cross-type corresponding to our mating design, "dh6" (Broman et al. 2019). Whenever individuals underwent both exome capture and GBS, the GBS reads were used to generate markers for QTL mapping. To prepare the data, a control file was created using the function write_control_file() from R/qtl2, which specifies the cross-type for our population, the file names of the population and parental SNPs, the physical map coordinates for the SNPs, the phenotype file, the cross information file, which contains the number of meiosis used to generate each individual, and the parental alleles "AA" through "FF." Due to the high density of markers, a genetic map was approximated by converting each SNP's megabase pair position to centiMorgans using the B73 RefGen_v5 chromosomal genome length of 2,132 Mbp divided by the composite US-NAM genetic map length of 1,456.68 cM (Li et al. 2015). The control file and all materials needed for mapping are provided as Supplemental File 5.

Any line with segregating per se phenotypes had previously been removed from further analysis. To identify potential sample duplicates, the function compare_geno() was used to calculate marker matching for all pairwise comparisons, and any pair of individuals with >95% marker sharing was removed. Conditional genotype probabilities, or the true genotype underlying the observed markers, were calculated using an HMM in the function calc_genoprob(), with an error probability of 0.01 (Broman and Sen 2009, Appendix D). After calculating genotype probabilities, the maximum marginal probability of the parental haplotypes was calculated and the total number of crossover events per individual was identified using the function count_xo(). Crossover locations were estimated using the function locate_xo(). Lines with unusually high numbers of total crossovers could be the result of sample contamination during population development or maintenance, as the HMM cannot accurately deduce the correct underlying parental haplotypes in nonparental regions, and instead frequently switches back and forth among the parent haplotypes. Lines in subset A with more than 150 crossovers or lines in subset B with more than 250 crossovers were removed from further analysis.

After quality control, 656 individuals remained with phenotypes and genotypes for mapping purposes (Supplementary Table 1). The genotype probabilities were used to calculate a kinship matrix, so the analysis could account for the relatedness between individuals using the "leave one chromosome out" method, which uses a kinship matrix derived from all other chromosomes except the chromosome under study to allow for a random polygenic effect (Yang et al. 2014). Next, single marker analysis was performed using a linear mixed model with the kinship matrix as a covariate to find associations between genotype and phenotype. Log of odds (LOD) thresholds were determined as the 95th percentile LOD score after 1,000 permutations of the founder probabilities using the function scan1perm() (Churchill and Doerge 1994; Cheng and Palmer 2013). Bayesian credible intervals for QTL peaks were calculated using the function find_peaks(), with LOD thresholds specific to each phenotype and probability of 0.95. To declare 2 QTL under 1 large peak, the LOD threshold was required to drop by at least 5. Chromosome-wide QTL best linear unbiased predictor (BLUP) effects were calculated using the function scan1blup(), and single locus BLUP effects were estimated using fit1() with "blup=T."

In addition to single marker QTL mapping, we also performed SNP association using the R/qtl2 function scan1snps(), with the same kinship matrix as previously described provided to account for population structure. Finally, not all DH lines included in the per se mapping were used to make the hybrid populations. To account for this difference in sampling between the per se traits and the hybrid traits, the sets of DH lines included in each hybrid population were used to repeat the mapping and

permutation procedures for each per se trait that corresponded to a hybrid trait.

Genomic prediction

To test the correlation between per se and hybrid phenotype based on the DH population per se genetics, we performed genomic prediction using the 100,000 SNP markers used for QTL mapping for both per se and hybrid prediction. We used the package R/rrBLUP to perform ridge regression on the marker effects, which is equivalent to calculating genomic estimated breeding values using a realized relationship matrix (Hayes *et al.* 2009; Endelman 2011). We used cross validation to train and test the models predicting per se and hybrid traits. We partitioned the phenotypic data into 5 segments and used 4 segments for training the model and the remaining portion for testing the model. We predicted the phenotypes for each of the 5 testing segments and calculated the correlation between the predicted and observed phenotypes, which comprised 1 replication. We repeated this process 100 times for each of the phenotypes. To indirectly predict the hybrid phenotypes from the parental per se phenotypes, we calculated the correlation between the testing set predicted per se phenotypes and the observed hybrid phenotypes.

Results

Phenotypic variation

Plant height and AnthGDU in the per se and hybrid populations showed normal distributions, and heritability ranged from 0.83 for SS-3IIH6 AnthGDU to 0.89 for SS-PHJ89 AnthGDU (Fig. 1; Supplementary Table 5). The genetic variance for per se, SS-3IIH6, and SS-PHJ89 AnthGDU was 2,781.6, 1,148.6, and 944.3 GDU^2, respectively, while the genetic variance for per se, SS-3IIH6, and SS-PHJ89 plant height was 386.3, 150.1, and 144.6 cm^2, respectively.

Similarly, the squared coefficient of variation for per se, SS-3IIH6, and SS-PHJ89 AnthGDU was 18.00, 9.24, and 7.33, while the squared coefficient of variation for per se, SS-3IIH6, and SS-PHJ89 PH was 124.93, 26.79, and 22.35, respectively. All traits except per se AnthGDU and SS-PHJ89 AnthGDU exhibited transgressive segregation, where one or more progeny DH lines had more extreme values than all the parents (Fig. 1). The parental line PHJ40 was the earliest flowering individual in the per se and SS-PHJ89 experiment.

Anthesis and silking were highly correlated within both DH lines and hybrids, ranging between Pearson's $r = 0.83$ for per se SilkGDU to per se AnthGDU to $r = 0.93$ for SS-3IIH6 SilkGDU to AnthGDU (data not shown). The correlation between per se AnthGDU and SS-3IIH6 AnthGDU was $r = 0.64$ and per se AnthGDU to SS-PHJ89 AnthGDU was $r = 0.66$ (Fig. 2, a and b). Correlation between AnthGDU for the 2 hybrid populations was higher at $r = 0.69$ (Fig. 2c). Plant height and ear height were also highly correlated within DH lines and hybrids. Correlations between plant height and ear height were $r = 0.79$ within both the per se and SS-3IIH6 populations and $r = 0.83$ within the SS-PHJ89 population (data not shown). Per se to hybrid plant height correlations were $r = 0.64$ between DH lines and SS-3IIH6 and $r = 0.71$ between DH lines and SS-PHJ89 (Fig. 2, d and e). Hybrid-to-hybrid plant height correlation was $r = 0.72$ (Fig. 2f). The high correlation between hybrids is expected, due to both the highly additive nature of flowering time and height and the relatedness between testers 3IIH6 and PHJ89.

On average, the SS-3IIH6 population was 71.5 cm taller and shed pollen 90.2 GDU earlier than its DH counterparts, and the SS-PHJ89 population was 82.0 cm taller and shed pollen 101.1 GDU earlier than its DH founders. Finally, height and flowering were also correlated within populations, where $r = 0.35, 0.41$, and 0.59 for the per se, SS-3IIH6, and SS-PHJ89 populations, respectively (Supplementary Fig. 1).
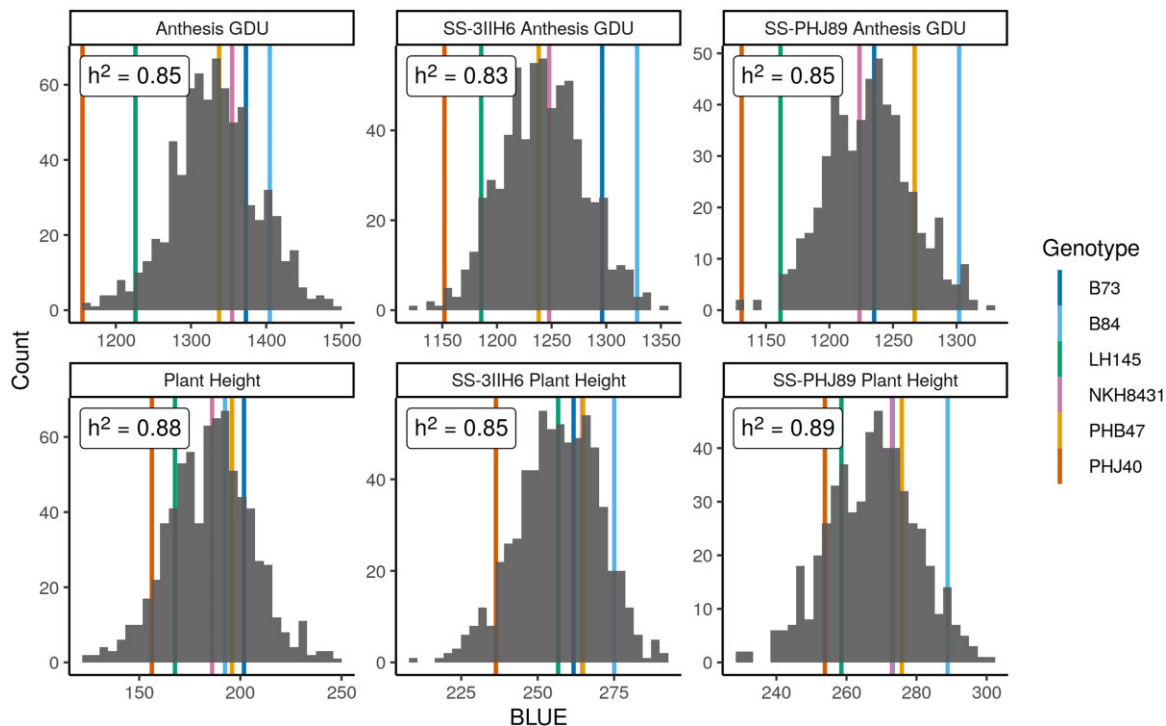

Fig. 1. Distributions of phenotypic BLUEs and heritabilities. Distributions for anthesis growing degree units (GDU) and plant height for the UW-MAGIC-SS per se population, SS-3IIH6 hybrid population, and SS-PHJ89 hybrid population. Trait heritabilities are in the upper left of each plot. Population parent BLUEs are plotted as colored lines behind each distribution.
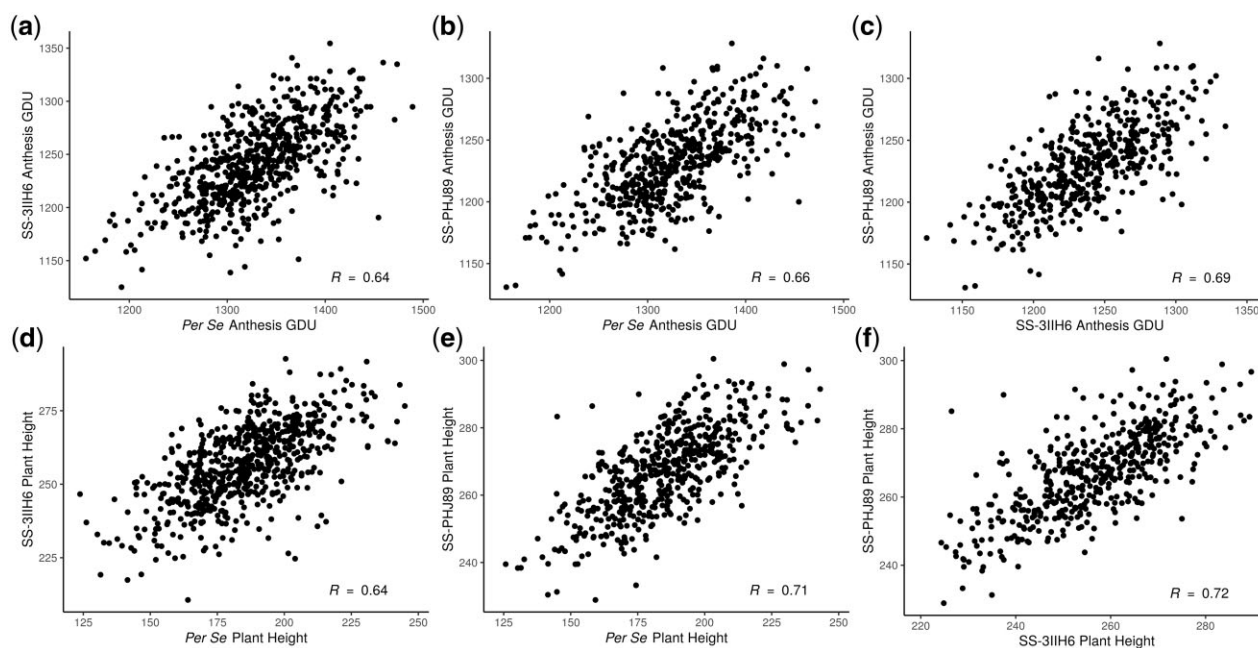
Fig. 2. Phenotypic correlations between populations for flowering time (a, b, c) and plant height (d, e, f). Scatterplots of BLUEs demonstrate the positive correlation within traits, between populations. Pearson correlations are shown in the lower right.

Practical haplotype graph

The 39,035 B73 RefGen_v5 annotated gene models were used as initial reference ranges, and after collapsing overlapping ranges, 36,399 genic ranges remained, and 36,401 intergenic ranges were inserted between genic ranges for a total of 72,800 ranges. The average genic range width was 4,755 bp, while the average intergenic range width was 53,811 bp. The theoretical maximum number of haplotypes per reference range is 6, which represents either all inbreds having sequence that aligns to the reference (including reference to reference alignment), or 5 inbreds that have alignment with the reference and 1 with a missing haplotype. Not all assemblies had sequence that aligns to every range owing to structural variation between the parental genomes. Each parental assembly had different numbers of total haplotypes aligning to B73, from 51,070 haplotypes for PHJ40 to 66,890 for B84. PHJ40 is known to be more structurally diverse from the other founders (Bornowski *et al.* 2021), and the next lowest number of aligned haplotypes was 62,144 for LH145. After collapsing haplotypes into consensus sequences, the average number of haplotypes per PHG reference range was reduced from 5.7 to 3.3 (Fig. 3a). Identity by descent relationships are present between all of the lines due to their common heritage from the BSSS, and these relationships are strongest between B73 and B84, B73 and NKH8431, and NKH8431 and LH145. Consensus parental and population haplotype identification numbers are presented in Supplementary Table 6.

Population genetic characteristics

MDS confirmed the lack of population structure within our population (Fig. 3b). The parental inbred lines fell on the perimeter of the point cloud, with no discernable clustering of progeny individuals. Allele frequency distributions for the major and minor alleles appeared as expected, with peaks near 1/6 and 2/6, corresponding to private and 2-way sharing of alleles within the parents, respectively (Fig. 3c). The founder probabilities and the total number of observable crossovers were calculated using R/qtl2. The 2 population subsets had overlapping distributions for

the total number of crossovers per individual. While examining the locations and total numbers of crossovers present within individuals, we found some areas of the genome in certain individuals contained unusually high numbers of crossovers. Such areas indicated that the HMM failed to choose a single founder for the area, and instead rapidly switched between founders. While some individuals had high total genome wide incidence of crossovers, which indicates a sample mix-up, some lines had isolated areas of high crossover in only a few regions. Small areas of high crossover could be caused by several factors, including residual heterozygosity in the founder inbreds, introgression from the DH inducer (Li *et al.* 2009), contamination during population development from an inbred closely related to one of the founders, or technical issues during the SNP calling pipeline. In addition, using a PHG with imputation to generate SNPs for the population forced each individual to have haplotypes only from the population founders which complicates identifying areas of inducer introgression or contamination. Most importantly, QTL mapping results did not change significantly between the raw, full set of lines and the cleaned, reduced set of lines filtered for high total crossovers (150 crossovers for subset A, 250 crossovers for subset B), indicating that our results were robust to this low level of uncertainty.

After removing individuals with high numbers of total crossovers and the other quality filters, the subset A (4 total meioses to generate DH lines) had an average of 60.7 crossovers, while subset B (6 total meioses to generate DH lines) had an average of 99.9 crossovers (Fig. 3d). The parental haplotypes for a set of 8 population individuals revealed a mosaic of the founder genotypes (Supplementary Fig. 2). The top row of individuals belongs to the subset A and showed longer parental haplotypes than the bottom row of individuals, which belong to subset B. In many individuals, there were chromosome sections plotted in white, which corresponded to areas where the founder probabilities did not rise above 0.5. This is expected, due to the related nature of the population founders and the segments of identity by descent between them. For example, large stretches of identity by descent
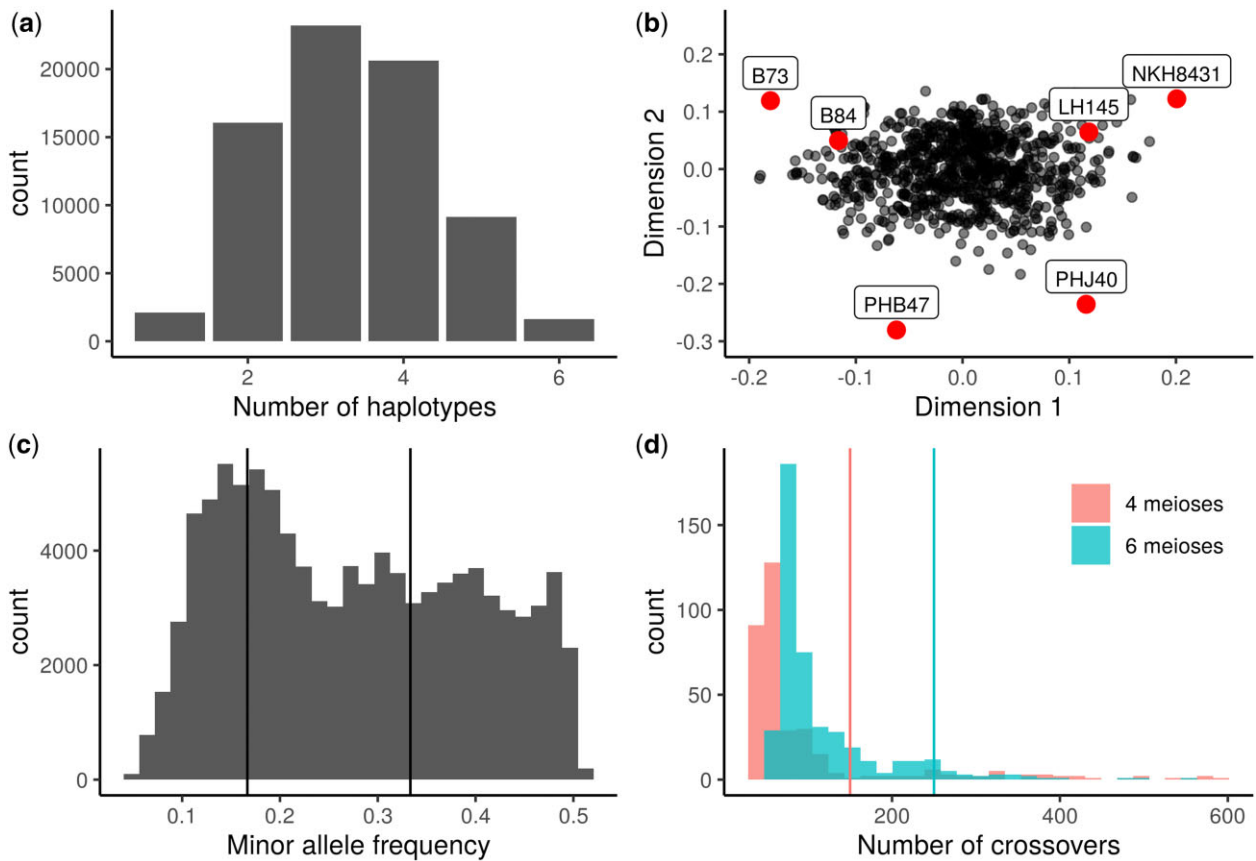
Fig. 3. Population genetic characteristics. a) Distribution of the number of consensus haplotypes found per reference range. b) Multidimensional scale plot using 1.8 million genic SNPs, with the population parents plotted in red. c) Distribution of the minor allele frequencies for 100,000 filtered numeric SNPs, with vertical lines plotted at expected peaks of 1/6 and 2/6. d) Histogram of the number of crossovers per individual for the 2 population subsets prior to filtering lines with high total crossovers. Six lines with more than 600 crossovers are not included. Vertical lines indicate the thresholds used for discarding lines at 150 crossovers for subset A (generated using 4 meioses) and 250 crossovers for subset B (generated using 6 meioses).

between B73 and B84 due to their selection out of the BSSS would make assigning population haplotypes to either of the parents difficult, and this issue is compounded by the presence of BSSS lines in the pedigrees of the other population parents. After removing individuals with high crossovers, some regions of local high crossover frequency remained, potentially due to introgression from the DH inducer which has been previously observed (Li *et al.* 2009) or possible factors such as residual heterozygosity in founder inbreds.

QTL mapping
QTL mapping and SNP association
To analyze flowering time and plant height, we took both a QTL mapping and SNP association approach. QTL mapping through single marker analysis as implemented by R/qtl2 relies on linear regression of the phenotypes on the matrix of founder probabilities, while SNP association regresses the phenotypes on the biallelic marker states. We found high concordance between QTL mapping and association analysis, where the most significant loci were identified for all traits by both approaches (Supplementary Figs. 3 and 4). Thus, we will refer to the QTL mapping results to represent our findings.

Flowering time
Mapping for AnthGDU revealed several significant peaks across the 10 chromosomes in the WI-SS-MAGIC DH population (Fig. 4a; Supplementary Fig. 5). The most significant peaks

appeared on chromosome 3 at 156.3, 163.1, and 168.5 Mbp and on chromosome 8 at 127.9 Mbp (Supplementary Table 7). Peaks for anthesis and silking highly colocalized, which is expected due to the high correlation of the phenotypic values at $r = 0.83$ (Supplementary Fig. 3). In the hybrids, the large significant peak on chromosome 8 disappeared in the SS-PHJ89 population but remained significant in the SS-3IIH6 population (Fig. 4, b and c). We calculated BLUP QTL effects for per se AnthGDU on chromosomes 3 and 8 and found allelic series at the significant loci on both chromosomes (Fig. 5). On chromosome 3, PHB47 provided the early flowering allele and LH145 provided the late flowering allele, while on chromosome 8 PHJ40 provided the early allele, and B73 and B84 provided later alleles. It is notable that LH145 was the second earliest parent of the population and PHB47 flowered near the mean of the population, demonstrating that alleles for early and late flowering segregate within the parents. Using a single QTL model to fit the BLUP effects for the chromosome 3 peak at 163,105,981 bp, the most extreme alleles from the parents showed a -27.2 ± 8.6 GDU effect for PHB47 and $+22.6 \pm 8.9$ GDU effect for LH145. For the peak on chromosome 8 at 127,898,534 bp, the most extreme effects were -24.4 ± 8.9 GDU from PHJ40 and $+17.4 \pm 8.9$ GDU from B73.

Plant height
Like flowering time, many significant peaks were also found for plant and ear height, such as on chromosomes 1, 2, 3, and 10
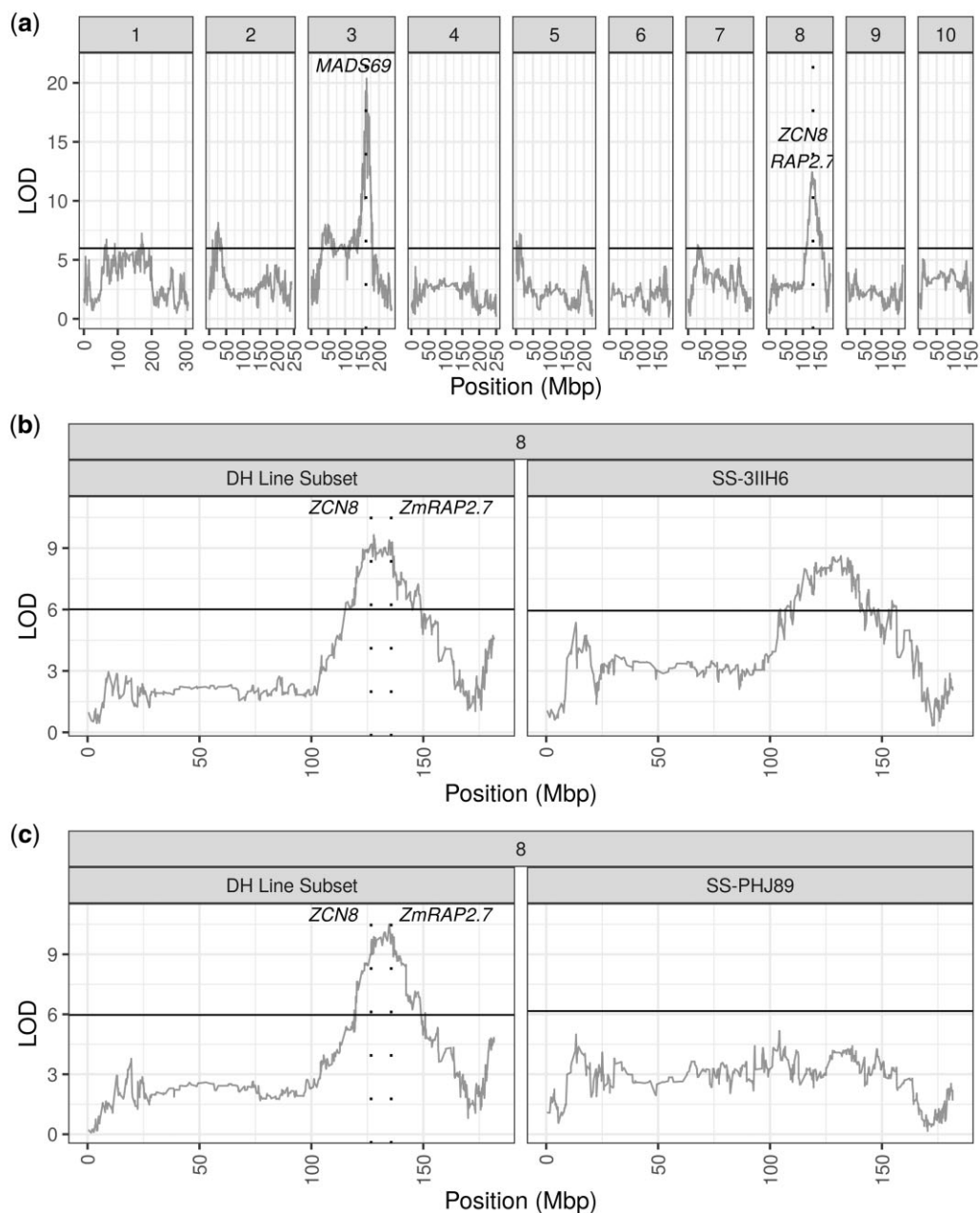
Fig. 4. Anthesis GDU QTL mapping. Population specific LOD scores are plotted for each panel. Dashed vertical lines show known flowering time genes. a) QTL peaks for the per se population for each of the 10 chromosomes. b) QTL peaks for chromosome 8 of the SS-3IIH6 population and the DH lines that were used to generate the population. c) QTL peaks for chromosome 8 of the SS-PHJ89 population and the DH lines that were used to generate the population.

(Fig. 6a; Supplementary Fig. 5 and Supplementary Table 7). Fewer loci colocalized for plant and ear height compared with AnthGDU and SilkGDU (Supplementary Fig. 4). A peak appeared for plant height on chromosome 6 at 105.8 Mbp in the SS-3IIH6 population that was not present in the per se or SS-PHJ89 population (Fig. 5b). We investigated the parental effects of the peak on chromosome 6 at 105,826,214 bp for both hybrid populations and found that the LH145 allele had an effect of $+3.6 \pm 1.7$ cm, while the B73 allele had an effect of -4.9 ± 2.0 cm in the SS-3IIH6 population (Supplementary Fig. 6). Here again, per se B73 was the tallest of the parents while per se LH145 was the second shortest and their allelic effects were opposite of their overall phenotypes, but their hybrid phenotypes were both closer to the population mean. For comparison, the insignificant chromosome 6 locus in

the per se and SS-PHJ89 populations showed no such differentiation between the parents (Supplementary Fig. 5). The genetic variance for plant height in the SS-3IIH6 population was 151.1 cm^2, so the allelic effects were a small proportion of the total variance.

Genomic prediction

Because information on the DH lines was available before hybrid test crosses were made, we tested the predictive abilities of several direct and indirect genomic prediction models (Fig. 7). As expected, the most successful models were those that were trained on the data that were most directly related to the predicted set, such as prediction within the hybrid SS-PHJ89 set and within the SS-3IIH6 set for plant height ($r = 0.63$ and $r = 0.60$, respectively) and prediction within the per se set for anthesis
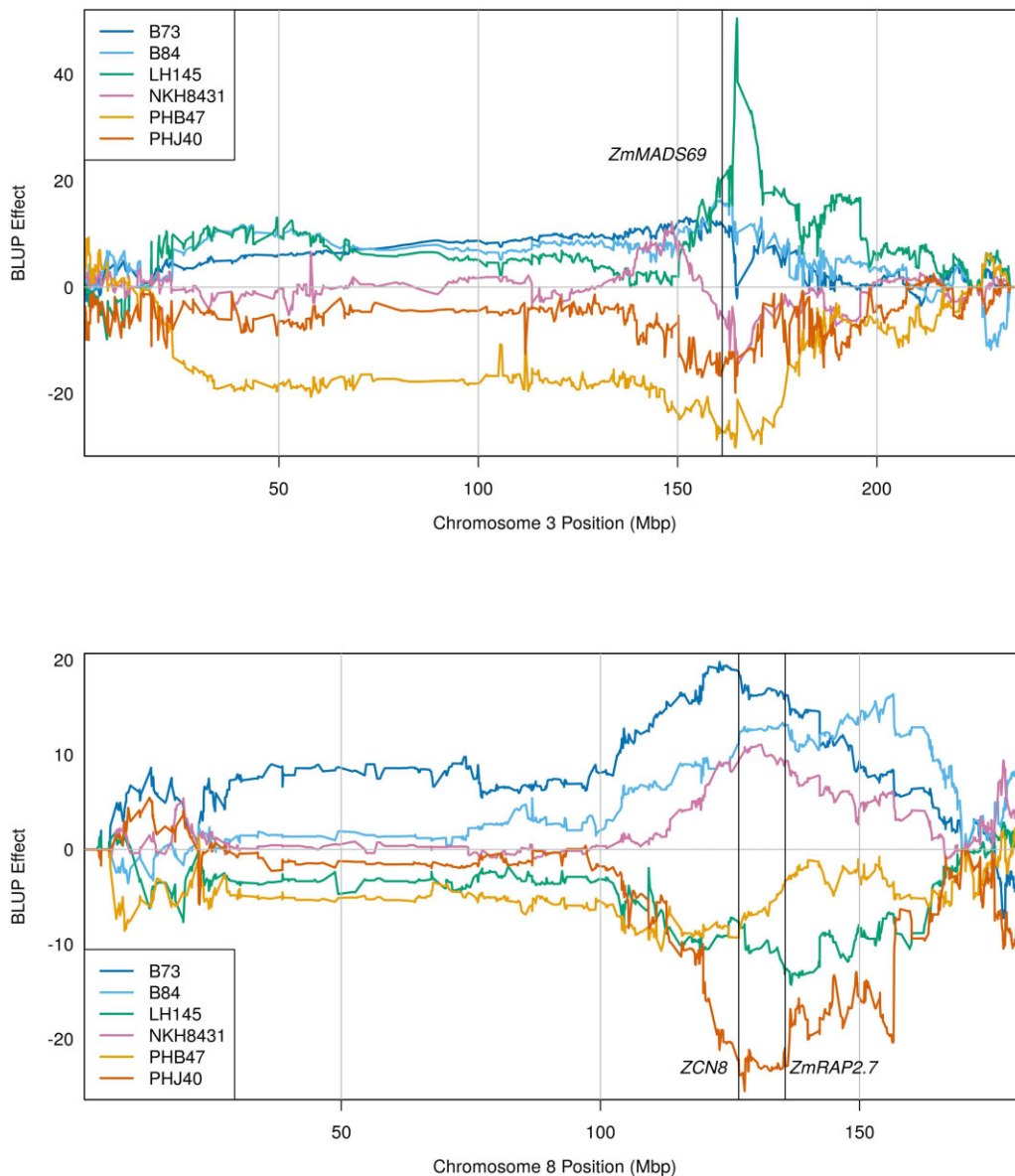
Fig. 5. Founder anthesis GDU QTL BLUP effects. BLUP effects for each parental contribution are plotted for the 2 chromosomes containing the most significant peaks for flowering time. Vertical lines are plotted denoting 3 major flowering time loci.

($r = 0.62$). Predictive abilities between test cross populations were moderate, with AnthGDU predictive abilities for SS-3IIH6 to SS-PHJ89 and vice versa of $r = 0.55$ and 0.54, and plant height at $r = 0.58$ and 0.53, respectively. The correlations of the indirect predictions of per se to hybrid phenotypes were lower, but still greater than $r = 0.49$. It is important to note that correlations do not consider the difference in scale between the per se and hybrid populations and cannot account for the population mean heterotic effect on both flowering time and plant height between the populations. Finally, we wanted to test the feasibility of using predicted per se data to discard DH lines from our breeding program that either are too tall or flower too late for our environment. We compared the predicted per se AnthGDU and per se plant height values to their observed values, and colored DH lines based on their status in the top 15th percentile for either the predicted or observed value (Supplementary Fig. 7). We maintained this color scheme when plotting the DH line's observed hybrid values to assess the combination of genomic prediction ability

and tester response. Overall, we found that the DH lines in the top 15th percentile for the predicted trait but not for the observed trait tended to be the DH lines that would make hybrids that are satisfactory to our breeding program's needs, while DH lines that were in the top 15th percentile of observed values tended to have higher hybrid values. These results are expected, especially considering the high correlations between per se and hybrid phenotypes and the lower predictive ability of the per se to hybrid models.

Discussion
QTL mapping in multiparent populations

Several multiparent populations have been developed in maize, including MAGIC populations from Italy and Spain (Dell'Acqua *et al.* 2015; Jiménez-Galindo *et al.* 2019), 4-parent populations from China and the USA (Ding *et al.* 2015; Mahan *et al.* 2018), and nested association mapping populations from the USA, China,
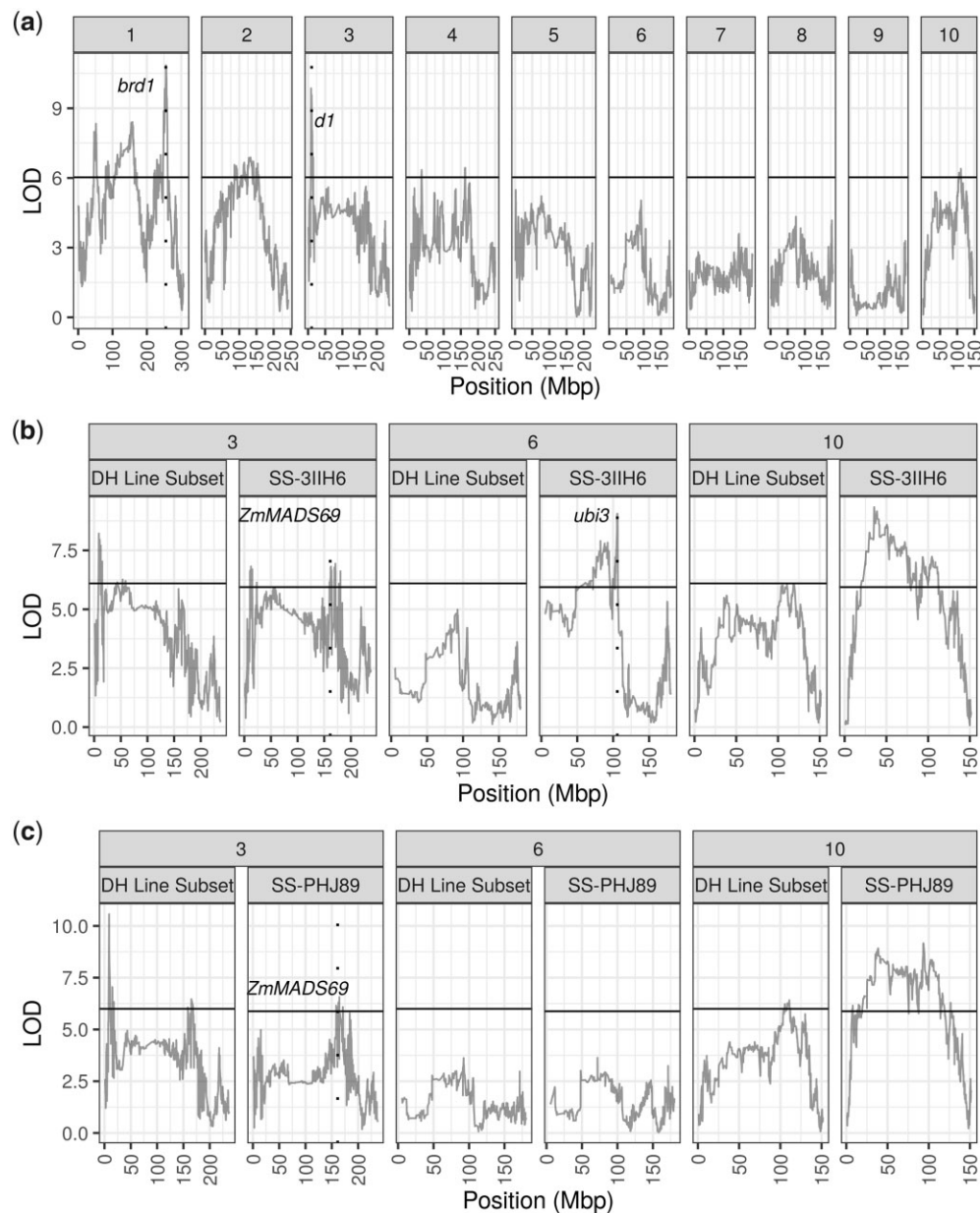
Fig. 6. Plant height QTL mapping. Population specific LOD scores are plotted for each panel. Dashed vertical lines show known height genes. a) QTL peaks for the per se population for each of the 10 chromosomes. b) QTL peaks for 3 chromosomes of the SS-3IIH6 population and the DH lines that were used to generate the population. c) QTL peaks for 3 chromosomes of the SS-PHJ89 population and the DH lines that were used to generate the population.

and Europe (Yu *et al.* 2008; Bauer *et al.* 2013; Li *et al.* 2013; Giraud *et al.* 2017). The existing MAGIC, US-NAM, and CN-NAM populations use a variety of inbreds that sample the diversity of maize genetics, and the European NAM populations focus on the Dent and Flint heterotic groups in addition to factorial crosses made between recombinant inbred lines. Our population concentrates the founders within the Stiff Stalk heterotic group. An advantage to focusing on the Stiff Stalk group is that maize breeding relies on recycling genetics within heterotic groups to make new parents and crossing parents between groups to make hybrids. In a factorial mating design between Flint and Dent multiparent populations, it was discovered that the majority of general combining ability QTL were specific to 1 heterotic group (Giraud *et al.* 2017; Seye *et al.* 2019). Thus, blending the genomes of parents within a single heterotic group vs across the diversity of maize

creates a more applicable population to study the subset of alleles present within Stiff Stalk seed parent germplasm released in North America. Breeding based on heterotic groups is expected to drive diverging allele frequencies between groups and constraining our mapping population to a single heterotic group allows us to examine the effects of these alleles on agronomic and yield related traits within their intended context. In addition, within the ex-PVP lines with combined Stiff Stalk admixture >50% from White *et al.* (2020) and including B73 and B84, 14.1% of rare Stiff Stalk alleles (minor allele frequency <0.05) are segregating within the WI-SS-MAGIC parents (data not shown, SNP data from Mazaheri *et al.* 2019). Recombining 6 parents increases the power to examine the effect of these rare alleles on phenotypes compared with a diversity panel. Mixing multiple founders takes advantage of historical recombination in addition to
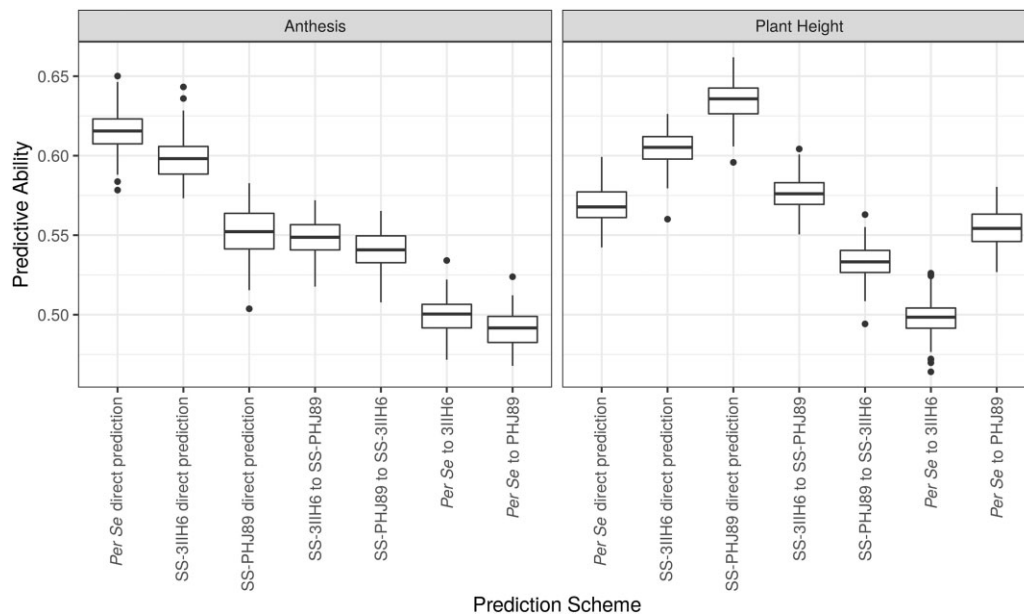
Fig. 7. Predictive abilities for direct and indirect genomic prediction models. Predictive abilities for 100 replications of each model. Direct models were trained using the population phenotype they would predict, while indirect models were trained with the per se or opposite hybrid population and used to predict each phenotype.

recombination introduced through population development. Multiple founders within a single population allows the study of allelic series at loci of interest, such as for AnthGDU on chromosomes 8 and 3 (Fig. 5).

QTL mapping in the WI-SS-MAGIC

Large efforts have been made by the plant research community to elucidate the control of complex traits such as flowering time and height. Several of the significant flowering time loci were near the location of other known flowering time genes. For example, chromosome 3 contains *ZmMADS69*, also known as *Zmm22*, and chromosome 8 contains *ZmRap2.7* and *ZCN8*, as noted in Fig. 4a. All 3 genes are known to regulate flowering time (Guo *et al.* 2018; Liang *et al.* 2019). Despite the high correlations between per se and hybrid flowering, several QTL that were significant in the per se population lost their significance in one or both hybrid populations. The large peak on chromosome 8 containing *ZmRap2.7* and *ZCN8* was not significant in the SS-PHJ89 population, despite retaining its significance in the group of DH lines used to make the hybrid population (Fig. 4c). The same locus remained significant in the SS-3IIH6 population, albeit with a smaller LOD score (Fig. 4b). Loss of significance indicates a loss in variation, such that the tester may have a dominant allele that masks the variation within the DH population. This suggests that there are contrasting loci present between the 2 testers, where PHJ89 has a dominant locus relative to the per se population while 3IIH6 does not.

The most significant locus for plant height on chromosome 1 was located at 225.4 Mbp and it contained *brd1*, a gene which is involved in the brassinosteroid pathway and for which a mutant allele causes severe dwarfism (Makarevitch *et al.* 2012). Likewise, the most significant locus on chromosome 3 at 8.9 Mbp contained another gene discovered through mutational studies, *DWARF1* (*d1*), which is involved in the gibberellin pathway (Chen *et al.* 2014). Most interestingly, a peak on chromosome 6 at 105.8 Mbp appeared for plant height in the SS-3IIH6 population, but not in the SS-PHJ89 population (Fig. 5b). This peak is near *ubi3*,

previously found to be associated with height traits (Ding *et al.* 2017). Previous studies have identified an epistatic interaction between *ubi3* and *br2* (Xiao *et al.* 2021).

Ding *et al.* (2017), used a near isogenic line from the US-NAM family B73 × Tzi8 crossed to B73 to finemap the QTL to 95–96 Mbp on chromosome 6. Like our study, Xiao *et al.* (2021), found a plant height QTL near 95.8 Mbp on chromosome 6 within 1 test cross population but not in the inbred population, and provides a schematic outlining the epistatic derepression uncovered by this locus. In theory, there is the potential to study epistasis between more than 2 founders within a MAGIC population. For the WI-SS-MAGIC population, comparing the founder states for 2 loci results in 36 total digenic classes. We separated our population into these classes for the 2 most significant loci for per se AnthGDU and found the mean number of individuals per class was 14.8, with a range of 2–45 individuals (Supplementary Fig. 8). Smaller population size in some of the sets exacerbates this issue of power. We repeated the procedure for the SS-3IIH6 plant height loci on chromosome 10 and 6 and found a mean of 7.3 individuals per class, with a range of 0–17, and 11 classes had fewer than 5 observed individuals (Supplementary Fig. 9). The limited number of observations per digenic class restricts the ability to statistically evaluate interaction between loci.

Our results demonstrate that QTL detection depends on the genetics of the tester when mapping in hybrid populations. While it is possible that the absence of a signal in the hybrid population could be due to environmental or genotype by environment effects, the high heritabilities support the large role of genetic variation.

QTL mapping in DH lines and hybrids

Previous work in mapping QTL across testers has found high concordance between plant height QTL discovered in different test cross populations and minimal digenic epistasis, despite evidence for epistasis under generation means analysis (Lübberstedt *et al.* 1997; Melchinger *et al.* 1998). Tester relatedness also influences the ability to discover QTL, where a tester unrelated to the

population uncovers QTL for additive traits more effectively than related testers (Frascaroli *et al.* 2009). Another study of a biparental RIL population crossed to 4 testers found that mapping the mean test cross height was sufficient to identify shared loci between testers (Austin *et al.* 2001). Recent work by Xiao *et al.* (2021), examining heterosis for over 42,000 hybrids generated by crossing 1,428 multiparent lines with 30 testers found that epistasis plays a role in generating heterosis, contradicting previous work demonstrating the low impact of epistasis (Hinze and Lamkey 2003; Mihaljevic *et al.* 2005).

We documented our population's response to 2 testers to better understand the heterotic effect of Iodent (3IIH6) and Oh43 (PHJ89) type testers on the WI-SS-MAGIC population. Understanding per se phenotypes requires mapping in an inbred population, while understanding an inbred's response to a tester requires evaluating and mapping traits in the hybrid population. We found the hybrid populations to have less than half the variation of the per se population, which could indicate that nonadditive gene action is affecting the phenotypes. The interplay of dominant and recessive loci only manifests in the hybrid population, either creating or concealing phenotypic variation depending on the gene action of the trait. Our study found evidence for contrasting allelic states between the 2 testers in several regions of the genome based on disappearance and appearance of QTL, including a dominant locus for flowering time on chromosome 8 in PHJ89 compared with 3IIH6, and a putatively epistatic locus revealed for plant height in 3IIH6. Despite the strong positive correlation between the hybrid phenotypes, several loci were found in only one of the hybrid populations (Supplementary Fig. 5). Perfect correlation between the test cross phenotypes would lead to the discovery of the same QTL between the 2 populations, yet the deviation from a one-to-one relationship between the test cross phenotypes leads to the discovery of unique QTL in the hybrid populations. Choice of tester influences hybrid performance and QTL mapping results, as evidenced by studies previously described and our findings. Despite the high correlation between the phenotypes of the hybrid populations and the expected identity by descent between the 2 testers, unique QTL were discovered for each trait in each population.

Genomic prediction of hybrid phenotypes

In maize breeding programs, per se phenotypes are often available before hybrid varieties can be tested. Using per se and hybrid data from our study, we investigated the association between per se and hybrid flowering and height traits. We wanted to test the feasibility of predicting correlations of hybrid flowering time and height based on DH line measurements for the purposes of discarding lines that flower too late or are too tall for our breeding program. We also wanted to evaluate the predictive ability between the 2 hybrid populations as breeding programs often use multiple testers as materials advance through selection pipelines.

We found that the hybrids flowered earlier and were taller than their maternal DH parents, confirming heterotic relationships for flowering and height found in other studies (Flint-Garcia *et al.* 2009; Li *et al.* 2018). Previous studies have found increased predictive abilities when incorporating parental inbred information (Liang *et al.* 2018; Jarquin *et al.* 2019), and we also found moderate prediction abilities for hybrid flowering time and plant height when the models were trained using the per se data. This stands in contrast to work by Galli *et al.* (2020), who found that genomic predictive ability in a partial diallel of 49 lines decreased when including information about the parents from

genome wide association. As expected, the models with the highest predictive abilities were those that were trained on the data they were designed to predict, although we achieved predictive abilities between $r = 0.49$ and $r = 0.55$ for models predicting hybrid traits that were trained with per se data. Correlations between per se and hybrid populations do not consider the difference in magnitude between them, such as the average difference between per se and hybrid flowering of 90 GDU or difference in height of 71 cm. Heterosis due to small genome-wide effects produces a relatively uniform incremental decrease in flowering time and increase in height across all lines, while variation within inbreds and within hybrids is largely due to similar large effect QTL likely in combination with undetected small effect loci. These findings are consistent with the overlapping and nonoverlapping QTL that were found between the per se and hybrid populations because the difference between the predictive abilities for direct and per se to hybrid models cannot account for the dominance or epistatic effect of the tester at individual loci. In addition, the masking of per se QTLs within either of the hybrid populations is conceptually consistent with the lowered predictive ability of using per se data to predict hybrids. We also found that the errors between predicted and observed per se phenotypes were a source of selection error that led to discarding DH lines that would have generated acceptable hybrids.

Finally, we also used the highest associated SNP from each LOD peak as fixed effects in the genomic prediction model but found that including the fixed marker effects lowered the predictive ability compared with using only the realized relationship matrix (data not shown). This finding supports previously simulated results demonstrating that known genes are only beneficial to models when they are few in number and explain large proportions of the variance (Bernardo 2014).

Relevance to maize breeding

This method has applications in maize breeding because genomic prediction could be used to make selections prior to generating test cross seed for an entire population. Alternatively, a smaller subset of an inbred population could be grown as a model training set with several testers prior to generating larger hybrid populations. Genomic prediction could then be used to discard the poorest performing lines, which would increase genetic gain by increasing the selection intensity on the population. Overall, our results indicate that plant breeders should be less aggressive when using predicted per se data to predict hybrid performance because the errors in genomic prediction can lead to discarding hybrid lines incorrectly. Plant breeders must balance their selection for maize yield with the adaptation requirements and architectural risk for root or stalk lodging when developing new inbred lines, as demonstrated by including information for flowering time and plant height in this study. Flowering time and moisture at harvest are also indications of overall relative maturity, which is an important characteristic that plant breeders use to place varieties across geographies and that farmers use to balance risk and make planting time and cultivar decisions. Our results indicate that flowering time and height have high correlations between DH lines and hybrids within these DH line–tester combinations yet experience different profiles of QTL significance across the genome. While the goal of maize breeding efforts is to increase or protect hybrid yield, most genetic research efforts focus on using inbreds to study complex traits. Understanding how traits manifest in a parental inbred vs its hybrid progeny is a critical area of maize breeding and quantitative genetics research. For example, parental per se measures of grain yield have been

previously used to increase prediction ability of hybrid performance (Schrag *et al.* 2010). Deviations from the purely additive relationship of inbred flowering time or plant height to hybrid phenotype can be investigated to add to the underlying understanding of the gene action that supports genomic prediction.

Conclusions

In conclusion, several known loci were uncovered in different combinations within the per se and test cross sets of a MAGIC population. Dominance of 1 tester over the population caused the loss of a highly significant peak for anthesis, while the presence of the other tester revealed putative epistatic variation for plant height. The 6 parents of the population are all members of the Stiff Stalk heterotic group, which is the canonical source of seed parent germplasm in the USA. These lines represent the diversity of both the subheterotic groups within the Stiff Stalk pool and the major plant breeding entities operating in the 1970s and 1980s and are no longer under intellectual property protection. In addition to dissecting the genetic architecture of these complex traits, this study provides a description of a new population resource available to maize researchers. Multiparent populations are a unique mapping resource to study the effect of more than 2 parental alleles on quantitative traits, and they are a means to increase the diversity of alleles under study while managing minor allele frequency. Further, the genome assemblies of the 6 parents with annotation from a 5-tissue transcriptome atlas (Bornowski *et al.* 2021; Li *et al.* 2021) are available for study, which increases the variety of opportunities for maize researchers. This population could be used to assay the effect of the alleles present within the population on combining ability, adaptation, genotype by environment interaction, stability, and provide a new paradigm for studying traditional and genomic selection. The practicality of leveraging linkage mapping of highly polygenic traits to make selections within breeding programs has been limited in the past, especially for traits that follow an infinitesimal model such as maize height (Peiffer *et al.* 2014). Nevertheless, further study of individual loci can impact plant breeding through mutational studies made possible by gene editing, in addition to current efforts in commercial plant breeding accomplished through genomic selection.

Data availability

All supplementary tables and files have been uploaded to FigShare at: https://doi.org/10.25386/genetics.19439684. Supplementary file 1 contains supplemental methods; Supplementary File 2 contains summary statistics regarding the exome capture; Supplementary File 3 contains the exome capture probe coordinates; Supplemental File 4 is contains the unfiltered 1.8 million SNPs data; and Supplementary File 5 contains the control folder for mapping in R/qtl2, including marker maps, genotypes, phenotypes, and cross information. Supplementary Table 1 contains descriptions of the lines in the study; Supplementary Table 2 contains details about the field experiments; Supplementary Table 3 contains plot-based data; Supplementary Table 4 contains information about the stage 1 models used for calculating BLUE phenotypes; Supplementary Table 5 contains the BLUE phenotypes; Supplementary Table 6 contains the reference range haplotype IDs; and Supplementary Table 7 contains all significant QTL peaks. Raw exome capture and GBS sequence reads are available in the National Center for Biotechnology Information Short Read Archive under BioProjects PRJNA781987 and PRJNA781986, respectively.

Conflicts of interest

None declared.

Literature cited

Alter P, Bircheneder S, Zhou L-Z, Schlüter U, Gahrtz M, Sonnewald U, Dresselhaus T. Flowering time-regulated genes in maize include the transcription factor *ZmMADS1*. Plant Physiol. 2016;172(1): 389–404. doi:10.1104/pp.16.00285.

Austin DF, Lee M, Veldboom LR. Genetic mapping in maize with hybrid progeny across testers and generations: plant height and flowering. Theor Appl Genet. 2001;102(1):163–176. doi:10.1007/s001220051632.

Bauer E, Falque M, Walter H, Bauland C, Camisan C, Campo L, Meyer N, Ranc N, Rincent R, Schipprack W, *et al.* Intraspecific variation of recombination rate in maize. Genome Biol. 2013;14(9):R103. doi:10.1186/gb-2013-14-9-r103.

Baum ME, Archontoulis SV, Licht MA. Planting date, hybrid maturity, and weather effects on maize yield and crop stage. Agron J. 2019; 111(1):303–313. doi:10.2134/agronj2018.04.0297.

Bernardo R. Genomewide selection when major genes are known. Crop Sci. 2014;54(1):68–75. doi:10.2135/cropsci2013.05.0315.

Bornowski N, Michel KJ, Hamilton JP, Ou S, Seetharam AS, Jenkins J, Grimwood J, Plott C, Shu S, Talag J, *et al.* Genomic variation within the maize stiff-stalk heterotic germplasm pool. Plant Genome. 2021;14(3):e20114. doi:10.1002/tpg2.20114.

Bradbury PJ, Casstevens T, Jensen SE, Johnson LC, Miller ZR, Monier B, Romay MC, Song B, Buckler ES. The practical haplotype graph, a platform for storing and using pangenomes for imputation. bioRxiv; 2021 [accessed 2021 Oct 25]. doi: 10.1101/2021.08.27.457652.

Bradbury PJ, Zhang Z, Kroon DE, Casstevens TM, Ramdoss Y, Buckler ES. TASSEL: software for association mapping of complex traits in diverse samples. Bioinformatics. 2007;23(19):2633–2635. doi: 10.1093/bioinformatics/btm308.

Brohammer AB, Kono TJY, Springer NM, McGaugh SE, Hirsch CN. The limited role of differential fractionation in genome content variation and function in maize (*Zea mays* L.) inbred lines. Plant J. 2018;93(1):131–141. doi:10.1111/tpj.13765.

Broman KW, Gatti DM, Simecek P, Furlotte NA, Prins P, Sen Ś, Yandell BS, Churchill GA. R/qtl2: software for mapping quantitative trait loci with high-dimensional data and multiparent populations. Genetics. 2019;211(2):495–502. doi:10.1534/genetics.118.301595.

Broman KW, Sen Ś. A Guide to QTL Mapping with R/Qtl. New York: Springer; 2009.

Buckler ES, Holland JB, Bradbury PJ, Acharya CB, Brown PJ, Browne C, Ersoz E, Flint-Garcia S, Garcia A, Glaubitz JC, *et al.* The genetic architecture of maize flowering time. Science. 2009;325(5941):714–718. doi:10.1126/science.1174276.

Butler DG, Cullis BR, Gilmour AR, Gogel BG, Thompson R. Asreml-R reference manual version 4. Hemel Hempstead (UK): VSN International Ltd; 2017.

Cai H, Chu Q, Gu R, Yuan L, Liu J, Zhang X, Chen F, Mi G, Zhang F. Identification of QTLs for plant height, ear height and grain yield in maize (*Zea mays* L.) in response to nitrogen and phosphorus supply. Plant Breed. 2012;131(4):502–510. doi: 10.1111/j.1439-0523.2012.01963.x.

Chen Y, Hou M, Liu L, Wu S, Shen Y, Ishiyama K, Kobayashi M, McCarty DR, Tan B-C. The maize *DWARF1* encodes a gibberellin 3-oxidase and is dual localized to the nucleus and cytosol. Plant Physiol. 2014;166(4):2028–2039. doi:10.1104/pp.114.247486.

Cheng R, Palmer AA. A simulation study of permutation, bootstrap, and gene dropping for assessing statistical significance in the case of unequal relatedness. Genetics. 2013;193(3):1015–1018. doi:10.1534/genetics.112.146332.

Churchill GA, Doerge RW. Empirical threshold values for quantitative trait mapping. Genetics. 1994;138(3):963–971. doi:10.1093/genetics/138.3.963.

Colasanti J, Yuan Z, Sundaresan V. The *indeterminate* gene encodes a zinc finger protein and regulates a leaf-generated signal required for the transition to flowering in maize. Cell. 1998;93(4):593–603. doi:10.1016/S0092-8674(00)81188-5.

Cullis BR, Smith AB, Coombes NE. On the design of early generation variety trials with correlated data. JABES. 2006;11(4):381–393. doi: 10.1198/108571106X154443

Dekalb Plant Genetics. Corn "3IIH6"; 1994. [accessed 2021 Jul 15]. https://apps.ams.usda.gov/CMS/AdobeImages/009300087.pdf.

Dell'Acqua M, Gatti DM, Pea G, Cattonaro F, Coppens F, Magris G, Hlaing AL, Aung HH, Nelissen H, Baute J, *et al.* Genetic properties of the MAGIC maize population: a new platform for high definition QTL mapping in *Zea mays*. Genome Biol. 2015;16(1):167. doi: 10.1186/s13059-015–0716-z.

Ding J, Zhang L, Chen J, Li X, Li Y, Cheng H, Huang R, Zhou B, Li Z, Wang J, *et al.* Genomic dissection of leaf angle in maize (*Zea mays* L.) using a four-way cross mapping population. PLoS One. 2015;10(10):e0141619.doi:10.1371/journal.pone.0141619.

Ding X, Wu X, Chen L, Li C, Shi Y, Song Y, Zhang D, Wang T, Li Y, Liu Z, *et al.* Both major and minor QTL associated with plant height can be identified using near-isogenic lines in maize. Euphytica. 2017;213(1):21. doi:10.1007/s10681-016–1825-9.

Duvick DN, Cassman KG. Post–green revolution trends in yield potential of temperate maize in the north-central United States. Crop Sci. 1999;39(6):1622–1630. doi:10.2135/cropsci1999.3961622x.

Elshire RJ, Glaubitz JC, Sun Q, Poland JA, Kawamoto K, Buckler ES, Mitchell SE. A robust, simple genotyping-by-sequencing (GBS) approach for high diversity species. PLoS One. 2011;6(5):e19379. doi: 10.1371/journal.pone.0019379.

Endelman JB. Ridge regression and other kernels for genomic selection with R package rrblup. Plant Genome. 2011;4(3):250–255. doi: 10.3835/plantgenome2011.08.0024.

Ewels P, Magnusson M, Lundin S, Käller M. MultiQC: summarize analysis results for multiple tools and samples in a single report. Bioinformatics. 2016;32(19):3047–3048. doi:10.1093/bioinformatics/btw354.

Falconer DS, Mackay TFC. Introduction to Quantitative Genetics, 3th edn. New York (NY): John Wiley and Sons, Inc; 1989.

Flint-Garcia SA, Buckler ES, Tiffin P, Ersoz E, Springer NM. Heterosis is prevalent for multiple traits in diverse maize germplasm. PLoS One. 2009;4(10):e7433.doi:10.1371/journal.pone.0007433.

Frascaroli E, Canè MA, Pè ME, Pea G, Morgante M, Landi P. QTL detection in maize testcross progenies as affected by related and unrelated testers. Theor Appl Genet. 2009;118(5):993–1004. doi: 10.1007/s00122-008–0956-3.

Galli G, Alves FC, Morosini JS, Fritsche-Neto R. On the usefulness of parental lines GWAS for predicting low heritability traits in tropical maize hybrids. PLoS One. 2020;15(2):e0228724. doi: 10.1371/journal.pone.0228724.

Gardner KA, Wittern LM, Mackay IJ. A highly recombined, high-density, eight-founder wheat MAGIC map reveals extensive segregation distortion and genomic locations of introgression segments. Plant Biotechnol J. 2016;14(6):1406–1417. doi: 10.1111/pbi.12504.

Giraud H, Bauland C, Falque M, Madur D, Combes V, Jamin P, Monteil C, Laborde J, Palaffre C, Gaillard A, *et al.* Reciprocal genetics: identifying QTL for general and specific combining abilities in hybrids between multiparental populations from two maize (*Zea mays* L.) heterotic groups. Genetics. 2017;207(3):1167–1180. doi: 10.1534/genetics.117.300305.

Guo L, Wang X, Zhao M, Huang C, Li C, Li D, Yang CJ, York AM, Xue W, Xu G, *et al.* Stepwise cis-regulatory changes in ZCN8 contribute to maize flowering-time adaptation. Curr Biol. 2018;28(18):3005–3015.e4. doi:10.1016/j.cub.2018.07.029.

Hayes BJ, Visscher PM, Goddard ME. Increased accuracy of artificial selection by using the realized relationship matrix. Genet Res (Camb). 2009;91(1):47–60. doi:10.1017/S0016672308009981.

Hinze LL, Lamkey KR. Absence of epistasis for grain yield in elite maize hybrids. Crop Sci. 2003;43(1):46–56. doi:10.2135/cropsci2003.4600.

Huang C, Sun H, Xu D, Chen Q, Liang Y, Wang X, Xu G, Tian J, Wang C, Li D, *et al.* ZmCCT9 enhances maize adaptation to higher latitudes. Proc Natl Acad Sci U S A. 2018;115(2):E334–E341. doi: 10.1073/pnas.1718058115.

Hung H-Y, Shannon LM, Tian F, Bradbury PJ, Chen C, Flint-Garcia SA, McMullen MD, Ware D, Buckler ES, Doebley JF, *et al.* ZmCCT and the genetic basis of day-length adaptation underlying the postdomestication spread of maize. Proc Natl Acad Sci U S A. 2012;109(28):E1913–E1921. doi:10.1073/pnas.1203189109.

Huynh B-L, Ehlers JD, Huang BE, Muñoz-Amatriaín M, Lonardi S, Santos JRP, Ndeve A, Batieno BJ, Boukar O, Cisse N, *et al.* A multiparent advanced generation inter-cross (MAGIC) population for genetic analysis and improvement of cowpea (*Vigna unguiculata* L. Walp.). Plant J. 2018;93(6):1129–1142. doi:10.1111/tpj.13827.

Jarquin D, Howard R, Liang Z, Gupta SK, Schnable JC, Crossa J. Enhancing hybrid prediction in pearl millet using genomic and/ or multi-environment phenotypic information of inbreds. Front Genet. 2019;10(1294):1294. doi:10.3389/fgene.2019.01294.

Jiménez-Galindo JC, Malvar RA, Butrón A, Santiago R, Samayoa LF, Caicedo M, Ordás B. Mapping of resistance to corn borers in a MAGIC population of maize. BMC Plant Biol. 2019;19(1):431. doi: 10.1186/s12870-019–2052-z.

Jin M, Liu X, Jia W, Liu H, Li W, Peng Y, Du Y, Wang Y, Yin Y, Zhang X, *et al.* ZmCOL3, a *CCT* gene represses flowering in maize by interfering with the circadian clock and activating expression of *ZmCCT*. J Integr Plant Biol. 2018;60(6):465–480. doi:10.1111/jipb.12632.

Khush GS. Green revolution: the way forward. Nat Rev Genet. 2001; 2(10):815–822. doi:10.1038/35093585.

Kover PX, Valdar W, Trakalo J, Scarcelli N, Ehrenreich IM, Purugganan MD, Durrant C, Mott R. A multiparent advanced generation inter-cross to fine-map quantitative traits in *Arabidopsis thaliana*. PLoS Genet. 2009;5(7):e1000551. doi:10.1371/journal.pgen.1000551.

Li C, Li Y, Sun B, Peng B, Liu C, Liu Z, Yang Z, Li Q, Tan W, Zhang Y, *et al.* Quantitative trait loci mapping for yield components and kernel-related traits in multiple connected RIL populations in maize. Euphytica. 2013;193(3):303–316. doi:10.1007/s10681-013–0901-7.

Li C, Yongxiang L, Bradbury PJ, Wu X, Shi Y, Song Y, Zhang D, Rodgers-Melnick E, Buckler ES, Zhang Z, *et al.* Construction of high-quality recombination maps with low-coverage genomic sequencing for joint linkage analysis in maize. BMC Biol. 2015;13(1): 78. doi:10.1186/s12915-015–0187-4.

Li L, Xu X, Jin W, Chen S. Morphological and molecular evidences for DNA introgression in haploid induction via a high oil inducer CAUHOI in maize. Planta. 2009;230(2):367–376. doi: 10.1007/s00425-009–0943-1.

Li Z, Coffey L, Garfin J, Miller ND, White MR, Spalding EP, N de L, Kaeppler SM, Schnable PS, Springer NM, *et al.* Genotype-by-environment interactions affecting heterosis in maize. PLoS One. 2018;13(1):e0191321. doi:10.1371/journal.pone.0191321.

Li Z, Zhou P, Della Coletta R, Zhang T, Brohammer AB, H O'Connor C, Vaillancourt B, Lipzen A, Daum C, Barry K, *et al.* Single-parent expression drives dynamic gene expression complementation in maize hybrids. Plant J. 2021;105(1):93–107. doi:10.1111/tpj.15042.

Liang Y, Liu Q, Wang X, Huang C, Xu G, Hey S, Lin H-Y, Li C, Xu D, Wu L, *et al.* ZmMADS69 functions as a flowering activator through the *ZmRap2.7-ZCN8* regulatory module and contributes to maize flowering time adaptation. New Phytol. 2019;221(4):2335–2347. doi:10.1111/nph.15512.

Liang Z, Gupta SK, Yeh C-T, Zhang Y, Ngu DW, Kumar R, Patil HT, Mungra KD, Yadav DV, Rathore A, *et al.* Phenotypic data from inbred parents can improve genomic prediction in pearl millet hybrids. G3 (Bethesda). 2018;8(7):2513–2522. doi:10.1534/g3.118.200242.

Lübberstedt T, Melchinger AE, Schön CC, Utz HF, Klein D. QTL mapping in testcrosses of European flint lines of maize: I. Comparison of different testers for forage yield traits. Crop Sci. 1997;37(3): 921–931. doi:10.2135/cropsci1997.0011183X003700030037x.

Mahan AL, Murray SC, Klein PE. Four-parent maize (FPM) population: development and phenotypic characterization. Crop Sci. 2018; 58(3):1106–1117. doi:10.2135/cropsci2017.07.0450.

Makarevitch I, Thompson A, Muehlbauer GJ, Springer NM. *Brd1* gene in maize encodes a brassinosteroid c-6 oxidase. PLoS One. 2012; 7(1):e30798.doi:10.1371/journal.pone.0030798.

Marçais G, Delcher AL, Phillippy AM, Coston R, Salzberg SL, Zimin A. MUMmer4: a fast and versatile genome alignment system. PLoS Comput Biol. 2018;14(1):e1005944.doi:10.1371/journal.pcbi.1005944.

Martin M. Cutadapt removes adapter sequences from high-throughput sequencing reads. Embnet J. 2011;17(1):10–12. doi: 10.14806/ej.17.1.200.

Mascher M, Richmond TA, Gerhardt DJ, Himmelbach A, Clissold L, Sampath D, Ayling S, Steuernagel B, Pfeifer M, D'Ascenzo M, *et al.* Barley whole exome capture: a tool for genomic research in the genus *Hordeum* and beyond. Plant J. 2013;76(3):494–505. doi: 10.1111/tpj.12294.

Mazaheri M, Heckwolf M, Vaillancourt B, Gage JL, Burdo B, Heckwolf S, Barry K, Lipzen A, Ribeiro CB, Kono TJY, *et al.* Genome-wide association analysis of stalk biomass and anatomical traits in maize. BMC Plant Biol. 2019;19(1):1–17. doi: 10.1186/s12870-019–1653-x.

Melchinger AE, Utz HF, Schön CC. Quantitative trait locus (QTL) mapping using different testers and independent population samples in maize reveals low power of QTL detection and large bias in estimates of QTL effects. Genetics. 1998;149(1):383–403.

Mihaljevic R, Utz HF, Melchinger AE. No evidence for epistasis in hybrid and per se performance of elite European flint maize inbreds from generation means and QTL analyses. Crop Sci. 2005;45(6): 2605–2613. doi:10.2135/cropsci2004.0760.

Mikel MA. Genetic composition of contemporary U.S. commercial dent corn germplasm. Crop Sci. 2011;51(2):592–599. doi: 10.2135/cropsci2010.06.0332.

Muszynski MG, Dam T, Li B, Shirbroun DM, Hou Z, Bruggemann E, Archibald R, Ananiev EV, Danilevskaya ON. *delayed flowering1* encodes a basic leucine zipper protein that mediates floral inductive signals at the shoot apex in maize. Plant Physiol. 2006;142(4): 1523–1536. doi:10.1104/pp.106.088815.

Ogawa D, Nonoue Y, Tsunematsu H, Kanno N, Yamamoto T, Yonemaru J-I. Discovery of QTL alleles for grain shape in the Japan-MAGIC rice population using haplotype information. G3 (Bethesda). 2018;8(11):3559–3565. doi:10.1534/g3.118.200558.

Ongom PO, Ejeta G. Mating design and genetic structure of a multiparent advanced generation intercross (MAGIC) population of sorghum (*Sorghum bicolor* (L.) Moench). G3 (Bethesda). 2018;8(1): 331–341. doi:10.1534/g3.117.300248.

Pascual L, Desplat N, Huang BE, Desgroux A, Bruguier L, Bouchet J-P, Le QH, Chauchard B, Verschave P, Causse M. Potential of a tomato MAGIC population to decipher the genetic control of quantitative traits and detect causal variants in the resequencing era. Plant Biotechnol J. 2015;13(4):565–577. doi:10.1111/pbi.12282.

Peiffer JA, Romay MC, Gore MA, Flint-Garcia SA, Zhang Z, Millard MJ, Gardner CAC, McMullen MD, Holland JB, Bradbury PJ, Buckler ES. The genetic architecture of maize height. Genetics. 2014;196(4): 1337–1356. doi:10.1534/genetics.113.159152.

Pioneer Hi-Bred International Inc. Corn "PHJ89"; 1992. [accessed 2021 Jul 15]. https://apps.ams.usda.gov/CMS/AdobeImages/ 009100092.pdf.

Poland JA, Brown PJ, Sorrells ME, Jannink J-L. Development of high-density genetic maps for barley and wheat using a novel two-enzyme genotyping-by-sequencing approach. PLoS One. 2012; 7(2):e32253. doi:10.1371/journal.pone.0032253.

Pope R. Calculating Degree Days. Iowa State Univ Ext Outreach Integr Crop Manag [Internet]; 2008. [accessed 2021 Apr 22]. https://crops.extension.iastate.edu/cropnews/2008/04/calculating-degree-days.

R Core Team. R: A Language and Environment for Statistical Computing. 2018. R Foundation for Statistical Computing, Vienna, Austria. URL https://www.R-project.org/.

Rogers AR, Dunne JC, Romay C, Bohn M, Buckler ES, Ciampitti IA, Edwards J, Ertl D, Flint-Garcia S, Gore MA, *et al.* The importance of dominance and genotype-by-environment interactions on grain

yield variation in a large-scale public cooperative maize experiment. G3 (Bethesda). 2021;11(2). doi:10.1093/g3journal/jkaa050.

Romay MC, Millard MJ, Glaubitz JC, Peiffer JA, Swarts KL, Casstevens TM, Elshire RJ, Acharya CB, Mitchell SE, Flint-Garcia SA, *et al.* Comprehensive genotyping of the USA national maize inbred seed bank. Genome Biol. 2013;14(6):R55. doi:10.1186/gb-2013-14-6-r55.

Russell WA. PL-17, Maize. Crop Sci. 1972;12(5):721.

Russell WA. Registration of B84 parental line of maize. PL-50, Maize. Crop Sci. 1979;19(4):566.

Saghai-Maroof MA, Soliman KM, Jorgensen RA, Allard RW. Ribosomal DNA spacer-length polymorphisms in barley: Mendelian inheritance, chromosomal location, and population dynamics. Proc Natl Acad Sci U S A. 1984;81(24):8014–8018. doi:10.1073/pnas.81.24.8014.

Salas Fernandez MG, Becraft PW, Yin Y, Lübberstedt T. From dwarves to giants? Plant height manipulation for biomass yield. Trends Plant Sci. 2009;14(8):454–461. doi:10.1016/j.tplants.2009.06.005.

Salvi S, Sponza G, Morgante M, Tomes D, Niu X, Fengler KA, Meeley R, Ananiev EV, Svitashev S, Bruggemann E, *et al.* Conserved noncoding genomic sequences associated with a flowering-time quantitative trait locus in maize. Proc Natl Acad Sci U S A. 2007; 104(27):11376–11381. doi:10.1073/pnas.0704145104.

Sannemann W, Huang BE, Mathew B, Léon J. Multi-parent advanced generation inter-cross in barley: high-resolution quantitative trait locus mapping for flowering time as a proof of concept. Mol Breed. 2015;35(3):86. doi:10.1007/s11032-015–0284-7.

Schrag TA, Möhring J, Melchinger AE, Kusterer B, Dhillon BS, Piepho H-P, Frisch M. Prediction of hybrid performance in maize using molecular markers and joint analyses of hybrids and parental inbreds. Theor Appl Genet. 2010;120(2):451–461. doi:10.1007/s00122-009–1208-x.

Schwarz G. Estimating the dimension of a model. Ann Stat. 1978; 6(2):461–464.

Scott MF, Ladejobi O, Amer S, Bentley AR, Biernaskie J, Boden SA, Clark M, Dell'Acqua M, Dixon LE, Filippi CV, *et al.* Multi-parent populations in crops: a toolbox integrating genomics and genetic mapping with breeding. Heredity (Edinb). 2020;125(6):396–416. doi:10.1038/s41437-020–0336-6.

Seye AI, Bauland C, Giraud H, Mechin V, Reymond M, Charcosset A, Moreau L. Quantitative trait loci mapping in hybrids between Dent and Flint maize multiparental populations reveals group-specific QTL for silage quality traits with variable pleiotropic effects on yield. Theor Appl Genet. 2019;132(5):1523–1542. doi:10.1007/s00122-019–03296-2.

Stephenson E, Estrada S, Meng X, Ourada J, Muszynski MG, Habben JE, Danilevskaya ON. Over-expression of the photoperiod response regulator *ZmCCT10* modifies plant architecture, flowering time and inflorescence morphology in maize. PLoS One. 2019; 14(2):e0203728. doi:10.1371/journal.pone.0203728.

Tibbs Cortes L, Zhang Z, Yu J. Status and prospects of genome-wide association studies in plants. Plant Genome. 2021;14(1):e20077. doi:10.1002/tpg2.20077.

Troyer AF. Background of U.S. Hybrid Corn. Crop Sci. 1999;39: 601–626.

Troyer AF. Background of U.S. Hybrid Corn II: breeding, climate, and food. Crop Sci. 2004;44(2):370–380. doi:10.2135/cropsci2004.3700.

Wallace JG, Zhang X, Beyene Y, Semagn K, Olsen M, Prasanna BM, Buckler ES. Genome-wide association for plant height and flowering time across 15 tropical maize populations under managed drought stress and well-watered conditions in sub-Saharan Africa. Crop Sci. 2016;56(5):2365–2378. doi:10.2135/cropsci2015.10.0632.

Wang L, Zhou Z, Li R, Weng J, Zhang Q, Xinghua L, Wang B, Zhang W, Song W, Li X. Mapping QTL for flowering time-related traits under three plant densities in maize. Crop J. 2021;9(2):372–379. doi:10.1016/j.cj.2020.07.009.

Wang X, Wu L, Zhang S, Liancheng W, Ku L, Wei X, Xie L, Chen Y. Robust expression and association of *ZmCCA1* with circadian rhythms in maize. Plant Cell Rep. 2011;30(7):1261–1272. doi:10.1007/s00299-011–1036-8.

White MR, Mikel MA, Leon N, Kaeppler SM. Diversity and heterotic patterns in North American proprietary dent maize germplasm. Crop Sci. 2020;60(1):100–114. doi:10.1002/csc2.20050.

Xiao Y, Jiang S, Cheng Q, Wang X, Yan J, Zhang R, Qiao F, Ma C, Luo J, Li W, *et al.* The genetic mechanism of heterosis utilization in maize improvement. Genome Biol. 2021;22(1):148. doi:10.1186/s13059-021–02370-7.

Xu J, Liu Y, Liu J, Cao M, Wang J, Lan H, Xu Y, Lu Y, Pan G, Rong T. The genetic architecture of flowering time and photoperiod sensitivity in maize as revealed by QTL review and meta analysis. J Integr Plant Biol. 2012;54(6):358–373. doi:10.1111/j.1744–7909.2012.01128.x.

Yang J, Zaitlen NA, Goddard ME, Visscher PM, Price AL. Advantages and pitfalls in the application of mixed-model association methods. Nat Genet. 2014;46(2):100–106. doi:10.1038/ng.2876.

Yu J, Holland JB, McMullen MD, Buckler ES. Genetic design and statistical power of nested association mapping in maize. Genetics. 2008;178(1):539–551. doi:10.1534/genetics.107.074245.

Communicating editor: H. Daetwyler